Renewable Energy 145 (2020) 1578–1596

Contents lists available at ScienceDirect

Renewable Energy

journal homepage: www.elsevier.com/locate/renene

CO_2 emission reduction in the cement industry by using a solar calciner

Gkiokchan Moumin [a, *], Maximilian Ryssel [b], Li Zhao [b], Peter Markewitz [b], Christian Sattler [a], Martin Robinius [b], Detlef Stolten [b, c]

[a] Institute of Solar Research, Deutsches Zentrum für Luft- und Raumfahrt/German Aerospace Center (DLR), Linder Höhe, D-51147, Cologne, Germany
[b] Institute of Energy and Climate Research, Electrochemical Process Engineering (IEK-3), Forschungszentrum Jülich, D-52425, Juelich, Germany
[c] Chair for Fuel Cells, RWTH Aachen University, D-52056, Aachen, Germany

ARTICLE INFO

Article history:
Received 11 April 2019
Received in revised form
25 June 2019
Accepted 8 July 2019
Available online 10 July 2019

Keywords:
CO_2 emissions reduction
Solar cement plant
Solar calciner

ABSTRACT

This paper discusses the techno-economic potential of solar thermal calciner technology in the cement industry. On the basis of a solar calciner test rig built at the German Aerospace Center (DLR), a solar cement plant is designed and the heliostat field is calculated. The energy balance in the solar calciner is analyzed and different scenarios are investigated. The achievable CO_2 avoidance rate for solar cement plants for the considered scenarios lies between 14 and 17%. CO_2 avoidance costs are 118 EUR/t in a conservative base case and can be as low as 74 EUR/t depending on the chosen direct normal irradiation (DNI), reactor efficiency and solar multiple. A strong impact of the reactor efficiency on the costs was shown. Increasing the reactor efficiency by 15% points reduces the avoidance costs by 26%. Additionally, the CO_2 emission reduction potential is calculated for Spain through 2050. It was found that for solar calciners, replacing the fossil fuel in the conventional calciner, emission reductions in the Spanish cement industry range between 2 and 7% by 2050. Implementation of a controlled sequestration of the CO_2 in the solar calciner shows a big impact and emission reductions from 8 to 28% can be achieved.

1. Introduction

Global cement production accounts for 8% of anthropogenic carbon dioxide emissions [1] and 13% of global greenhouse gas emissions from industrial sources [2]. Today, all newly-built cement plants are dry process plants with cyclone preheaters and calciners and are considered state-of-the-art [3]. In the cement manufacturing process, there are two important chemical reactions: the calcination of cement raw meal at 900 °C and the subsequent sintering to produce the clinker at 1350–1500 °C [4]. The former takes place in the calciner where the following reaction takes place [5]:

$$CaCO_3(s) \rightarrow CaO(s) + CO_2(g),\ \Delta H_R = 3180\ \text{kJ/kg CaO at 25 °C}.$$

About half of the emissions during the cement production arise from this reaction [1]. The subsequent sintering, or clinkering, is performed in the rotary kiln [6]. Considering the recent increase in prices for CO_2 emission trading to close to 25 EUR/t [7], the implementation of solar thermal energy into the cement production process becomes more and more attractive.

Implementing the solar thermal energy into the cement plant would take place through a solar reactor in which heat is supplied via concentrated solar energy. Two different process designs for the solarization of the calcination step (Fig. 1), which are distinguished by the location of the solar reactor, are discussed in the literature [8–10]:

- Top of tower (TT) system: The solar reactor is placed on top of a tower. This option is considered superior, as optical losses are low compared to a beam down plant.
- Beam down (BD) system: The reactor is placed on the ground and the concentrated solar influx collected by the heliostat mirrors is concentrated on and reflected from a parabolic reflector on top of a tower down to the solar reactor. This approach is considered advantageous, as the solar reactor can be

* Corresponding author.
E-mail addresses: Gkiokchan.Moumin@dlr.de (G. Moumin), Maximilian.Ryssel@giz.de (M. Ryssel), l.zhao@fz-juelich.de (L. Zhao), p.markewitz@fz-juelich.de (P. Markewitz), Christian.Sattler@dlr.de (C. Sattler), m.robinius@fz-juelich.de (M. Robinius), d.stolten@fz-juelich.de (D. Stolten).

https://doi.org/10.1016/j.renene.2019.07.045

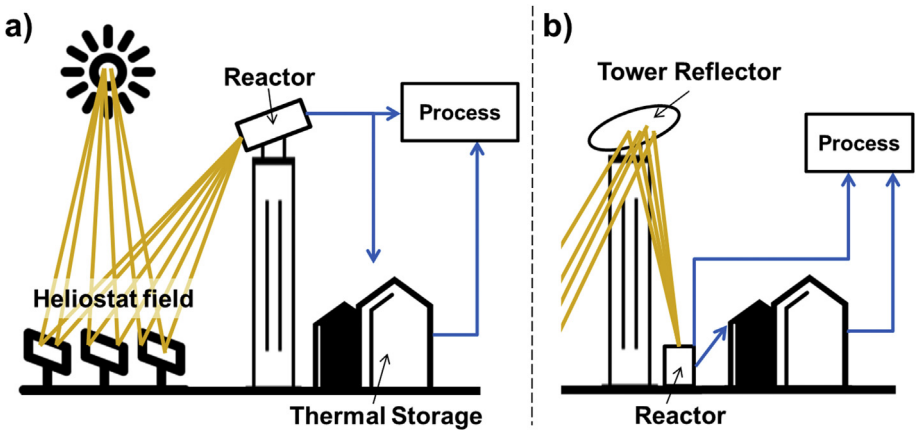

Fig. 1. a) Top-of-Tower (TT) and b) Beam-Down (BD) solar plant design based on Pitz-Paal, Buck et al. [11].

placed on the ground, where it is easily supplied with raw material and maintained. However, the losses of solar flux via the additional reflector are increased and the reflector requires a large additional investment. Due to this and its limitation in power make it inferior to the TT design.

In this paper, a system analysis is conducted to explore the solar thermal calciner technology. CO_2 emission projections for the clinker-producing industry and emission reduction potentials in Spain are investigated [12]. For the first time in literature an hourly DNI resolution is considered for the calculations. This is a much more precise approach instead of the usage of an average DNI for a specified time period. Furthermore, the number of solar towers and the heliostats are optimized based on the required nominal power. Lastly the storage size is taken as an additional parameter, showing, together with the hourly DNI, the optimum size to achieve maximum solarization of the process. As the solar thermal calcination reactor the concept of a lab-scale rotary kiln, tested at the DLR in Cologne [13,14], was chosen. During a holistic investigation, including of the literature, cement plant design, energetic analysis, scenarios exploration and economic evaluation was not carried out regarding this type of cement plant.

The paper is structured as follows: Section 2 includes a literature review that focuses on solar calcination reactors. Section 3 describes the basis of our calculations and assumptions. In section 4, the results are presented and discussed. Section 5 includes scenario calculations for Spain if conventional calciners are replaced by solar technology. Lastly, section 6 summarizes and concludes this work.

2. Solar calcination reactors in cement production

For the utilization of solar calcination reactors, several theoretical studies have been carried out and prototype reactors have been built and investigated [8–10,13,15–19].

2.1. Literature review

Imhof [17] assessed the economic potential of solarizing a 3000 t/d clinker plant. A hybrid process that includes a solar and fossil calciner was investigated. The solar irradiation is assumed to reach levels above 2000 kWh/m^{2}a and the calciner efficiency is set to 86%. Thermal storage was not included in the investigation. The author's analysis shows that 9% of CO_2 emissions and 28% of all fossil fuel inputs could be avoided in comparison to a conventional cement plant. In contrast to the rotary kiln reactor design investigated by Meier et al. [9,18], a falling particle receiver is used in which a particle curtain absorbs the solar incident power. It presumes that the particles are big enough to not be affected by the wind or that a mounted window will stay clean of depositions. This simple design is reflected in the very low reactor costs of only 0.6 MEUR. It is assumed that the reactor is built on top of the preheater tower and that the tower costs are hence mainly composed of reinforcement and enhancement costs. Against this premise, the CO_2 avoidance costs are found to be around 74 CHF/t_{CO2} (50 EUR_{2000}/t_{CO2}).

Meier et al. [8] conducted an economic study of a solar lime plant with a production capacity of 50 tons of lime per day. The reference plant's single shaft lime kiln is substituted by a solar reactor. Other parts of the plant are adopted from a conventional cement plant. Beam-down (BD) and top-of-tower (TT) process designs with 1, 5 and 25 MW_{th} solar incident power on the reactor, respectively, are investigated. For the plant location, the authors use a Direct Normal Irradiation (DNI) of 2300 kWh/m^2 and state that at least 500–600 W/m^2 of irradiation are necessary for plant start-up. For the economic analysis, only the major cost differences between the conventional and solar lime plant are considered. These are the heliostat field and tower costs, compound parabolic concentrator (CPC), kiln and land costs. For the calculation of the kiln costs, the authors only consider the cost difference between a conventional and solar reactor, resulting in capital cost savings for the 1 MW_{th} TT and BD systems, as well as the 5 MW_{th} BD system. The overall optical efficiency for the heliostat field is 61% for the top-of-tower and 52% for the beam-down configuration. The reactor's efficiency is assumed to reach 40–50% according to the authors' experimental findings [18]. The production costs for lime are 76 USD/t (68.4 EUR/t) in the best case and 118.7 USD/t (106.8 EUR/t) in the worst one. Furthermore, the payback time is calculated. Therefore, the authors assume that the lime produced in the solar plant is of a superior quality, achieving market prices of two times the conventionally-produced lime price (i.e., 120 USD/t; 108 EUR/t). Their results show that only the 25 MW_{th} plant achieves economic profitability, with a payback time of eight years. Major cost reductions are expected from the heliostat field costs, constituting 62% of the additional costs for the solar lime plant. For the plant investigated, 95% of the CO_2 emissions that would be emitted from the burning of fossil fuels are avoided. The authors propose that adequate future government subsidies and a rising CO_2 tax will facilitate the market introduction of solar lime plants in the future.

González and Flamant [10] conducted as a first approach a technological and economic feasibility study on a concentrated solar power hybrid (solar energy + fossil fuel) cement plant. The considered capacity was 3000 t/d of cement clinker. A fossil fuel

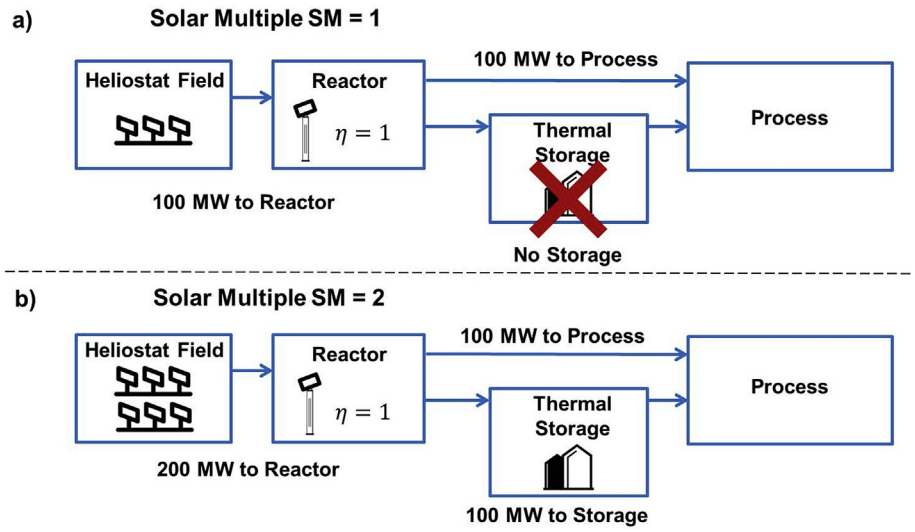

Fig. 2. Example for a 100 MW process supplied by a solar power plant with a solar multiple of a) SM = 1 and b) SM = 2.

substitution of the calciner in the range of 40–100% is discussed and evaluated. The DNI used for the evaluation is 2550 kWh/m^{2}a. A thermal storage silo using calcined hot raw meal at 900 °C (the calcination temperature) is proposed. The solar calciner is located at the top of the existing preheater tower, and hence only tower costs relating to reinforcement and meal transportation are considered. The solar reactor is operated for 9 h per day (every day, on average), producing calcined meal for the further cement production process, as well as for the thermal storage. The authors estimate the land utilization and equipment sizing by determining the process' heat and mass balances. For estimating the solar reactor costs, the authors derive an equation of scale from Meier et al.'s work [8]. However, the cost data used only represents the compound's parabolic concentrator (CPC) cost. Hence, the solar reactor costs are not considered in González and Flamant's work. From calculating the payback time and internal rate of return for the concentrated solar power (CSP) investment, the authors conclude that it is economically feasible to integrate such a technology in the cement production process. A separate calculation of the costs of the specific CO_2 avoidance costs is also not given for the amount of CO_2 avoided. In contrast to Meier et al.'s work [8], the authors assume a high overall optical efficiency of 79% (at nominal conditions), as well as thermal efficiencies of the solar calciner from 55 to 85%. Hence, their results show higher economic potential, with a payback time of six years in the best case scenario. The solar influx necessary to drive the reaction ranges between 94 MW_{sol} (40% substitution, 85% thermal reactor efficiency) to 363 MW_{sol} (100% substitution, 55% reactor thermal efficiency).

2.2. Thermal storage and solar multiple

DNI is only available for a fraction of hours per day and is largely dependent on the sun's position and weather (clouds, fog), resembling a Gaussian distribution as a graph over the course of an average day, peaking at the solar noon. However, to be able to supply heat during cloudy weather or at night, thermal storage systems must be implemented. Excess solar energy produced during the day can then be stored and utilized at night. Thermal storage systems thereby significantly improve the capacity factor and economic competitiveness of a solar power plant [20].

Current thermal storage systems consist of two storage tanks, molten salt as the storage medium (typically a mixture of sodium and potassium nitrate), heat exchangers, additional piping and pumps, etc. [11,21]. A brief overview of the status quo, trends and developments of thermal storage systems can be found in Pitz-Paal and Buck et al.'s work [11].

To be able to supply excess energy for storage, the heliostat field must be oversized with respect to the nominal heat capacity of the solar reactor [20,22]. This ratio, termed the 'Solar Multiple' (SM), is described by von Storch [22] "as the nominal thermal capacity of the receiver in relation to the nominal capacity of the subsequent process." In reality, solar plants without thermal storage are designed with an SM of 1.1–1.5 to cope with thermal losses [20].

A schematic solar plant with an SM of 1 and 2 is depicted in Fig. 2. Here, an exemplary process with a power demand of 100 MW is to be satisfied using a solar tower. For the sake of simplicity, a reactor efficiency of 100% is assumed. In case a) SM = 1, the reactor provides exactly 100 MW to the process in the design point, hence no energy can be stored. In case b) SM = 2, a larger reactor and larger heliostat field are able to provide 200 MW. Hence, 100 MW are directly used in the process and 100 MW are stored. Case b) will require higher investments due to the larger heliostat field, reactor and thermal storage. However, case b) will show a higher capacity factor compared to a).

2.3. Solar calcination reactors

At the DLR's Institute of Solar Research, in the framework of the H2020 SOLPART project, a solar rotary kiln calciner has been designed and tested in a solar simulator [14], depicted in Fig. 3.

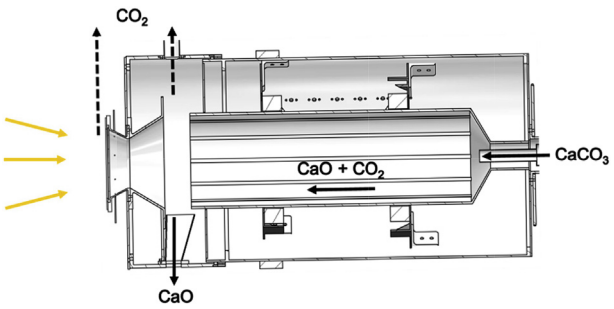

Fig. 3. Solar rotary kiln as a calciner used at the DLR.

Table 1
Performance parameters of solar calciner tested at DLR [14].

Parameter	Value	Unit
Raw meal flow tested	7.7	kg/h
Raw meal temperature at inlet	20	°C
Raw meal temperature at outlet	1000	°C
Calcination/conversion ratio	95	%
Input power	14.2	kW_{th}
Thermal efficiency	37	%
Start-up time	2	h

Feeding rates of 4–12.4 kg/h of raw cement meal were tested. For a material flow of 7.7 kg/h and an inlet temperature of 20 °C, a maximum temperature of 1000 °C at the outlet was reached with a conversion ratio of 95%. The input power was 14.2 kW_{th}, corresponding to a total efficiency, defining the energy uptake for the heating and reaction of the particles, of 37%. For the sake of simplicity, this total efficiency is defined in this work as the "thermal efficiency". About 2 h were necessary for heating up the reactor.

Table 1 summarizes the performance indicators.

Several reactors have been tested in the literature for the calcination of limestone [9,15,16,18,19,23], which is the main component of cement raw meal. However, up to now only defined particle size distributions were treated. While some reactors used particles bigger than 100 μm and hence avoided cohesion [9,15,18], others focussed on particles smaller than 100 μm but with prior sieving and a defined size range [16,19,23]. In the case of Moumin et al. the feedstock was obtained from a cement producer [14], which therefore provides a better basis for further studies. The particle size of the feedstock was <176 μm. Tests were performed in a solar rotary kiln, in which particles enter at the back and leave in the front. The reaction gas CO_2 was then extracted from the top and front of the reactor (see Fig. 3). A detailed literature review of the other discussed reactors can be found in Moumin et al. [14].

3. Modelling of the solar cement plant

This section provides a holistic analysis of the solar cement plant. Starting with the solar cement plant design (section 3.1), the energy requirements and CO_2 reduction possibility (section 3.2), heliostat field layout (section 3.3), DNI data sets used (section 3.4), underlying models and assumptions for operation, energetic and economic analysis (section 3.5 and 3.6) are given.

3.1. Solar cement plant design

Fig. 4 depicts the process design in this paper, similar to previous work [10]. The plant is operated in hybrid mode. Hence, in conventional, coal-fired operation, raw meal enters the preheater, from which it is fed to the calciner. The calcined meal is fed into the rotary kiln and sintered. In solar operation, the raw meal is heated up in the preheater and then transported to the solar calciner on top of the solar tower. The solar incident power at the reactor provides the necessary heat for the calcination and the calcined raw meal is then fed directly to the rotary kiln or thermal storage medium. Raw meal is stored at the outlet temperature from the solar calciner. If the solar calciner cannot provide sufficient raw meal for continuous rotary kiln operation, either the raw meal from the thermal storage is supplied to the kiln or the heat is supplied via the conventional calciner. As in the conventional cement plant, it is assumed that the flue gas is led in countercurrent to the clinker production process.

The largest existing solar power plants today achieve a solar

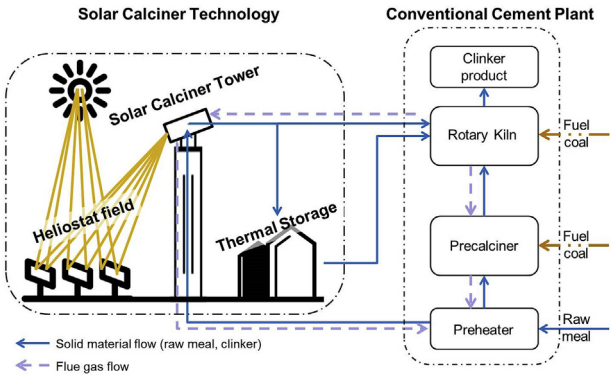

Fig. 4. Solar cement plant design.

incident power of around 600 MW_{sol} for surrounding fields (NOOR III, Morocco) [24]. However, the location investigated here is southern Spain, which is only suitable for northern fields. Hence, the maximum realistic solar field size assumed is 130 MW_{sol} of solar incident power for a single solar tower. If a higher incident power is necessary in the investigated case, the solar incident power is equally split on several smaller heliostat fields.

Furthermore, it is assumed that the maximum solar calciner size is 55 MW_{sol} of solar incident power. This takes into account that solar calciners designed as rotary kilns have an open inlet as apertures; if the solar calciner would be enlarged, the front opening would be increased, too. Hence, at some point upholding a high thermal efficiency while coping with an increasing false air input into the reactor would be ever more difficult.

If the solar incident power per tower is larger than 55 MW_{sol}, it is assumed that several solar calciners – of identical size – are placed on a solar tower.

3.2. Energy requirement and maximum CO_2 reduction

In this section, the thermal and solar energy requirements to power the cement plant calciner are determined using a heat balance. The maximum possible CO_2 reduction that can be achieved if the calciner is 100% solarized will also be examined.

3.2.1. Heat balance

In order to determine the size of the solar calciner, the heat balance for the reactor is calculated. Fig. 5 shows the relevant heat and mass streams. A detailed heat balance description can be found in Appendix A-C.

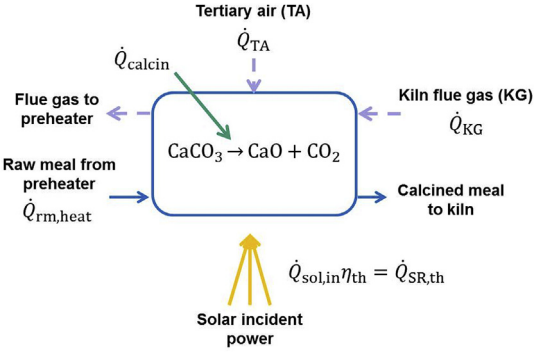

Fig. 5. Solar calciner heat balance.

3.2.2. Maximum CO_2 reduction potential

The maximum CO_2 reduction potential is achieved if 100% of the fossil energy in the calciner is substituted, i.e., a solarization rate of 100% is achieved. In this case, the CO_2 reduction equals:

$$\dot{m}_{CO_2,red,max} = \dot{m}_{CO_2,conv} - \dot{m}_{CO_2,sol,min} \quad (1)$$

The minimum CO_2 emissions of the solar cement process $\dot{m}_{CO_2,sol,min}$ are determined by the CO_2 content in the raw meal Y_{rm,CO_2} and the coal burned in the sintering rotary kiln $\dot{m}_{coal,kiln}$:

$$\dot{m}_{CO_2,sol,min} = Y_{rm,CO_2}\dot{m}_{rm} + \dot{m}_{coal,kiln}LHV_{coal}c_{CO_2} \quad (2)$$

The CO_2 emissions from the conventional process $\dot{m}_{CO_2,conv}$ are determined by the CO_2 content in the raw meal and the coal burned in the rotary kiln and calciner $\dot{m}_{coal,calcin}$:

$$\dot{m}_{CO_2,conv} = Y_{rm,CO_2}\dot{m}_{rm} + \dot{m}_{coal,kiln}LHV_{coal}c_{CO_2} + \dot{m}_{coal,calcin}LHV_{coal}c_{CO_2} \quad (3)$$

Hence, the CO_2 emission reduction by using a solar calciner instead of a conventional, coal fired reactor, is calculated from the fuel savings:

$$\dot{m}_{CO_2,red,max} = \dot{m}_{coal,calcin}LHV_{coal}c_{CO_2} \quad (4)$$

where c_{CO_2} is the specific CO_2 emission factor per unit of heat content of the fuel.

For details on the used data see table Table 13 in the appendix.

Using these equations, the CO_2 emissions in the conventional case are calculated as $m_{CO_2,conv}/m_{clinker} = 842\ kg_{CO_2}/t_{clinker}$. About 66% of these emissions are due to the calcination reaction. The remaining 34% are caused by the fuel used in the clinkering (about 13% points) and in the conventional calciner (about 21% points) [25,26]. The minimum emissions by utilizing the solar calciner equal $m_{CO_2,sol,min}/m_{clinker} = 665\ kg_{CO_2}/t_{clinker}$. Hence, the maximum CO_2 reduction in the case of a 100% calciner solarization by replacing the fossil fuel in the conventional calciner is equal to 21%. It is worth noting that the emissions due to the reaction are three times higher than the emissions due to the fuel consumption. Hence, the impact would be increased by a factor of four to 87% if a controlled separation of the CO_2 in the solar calciner is realized.

3.3. Heliostat field layout

From the solar incident power required for continuous operation of the solar cement plant, the heliostat field layout is determined using the DLR tool HFLCAL (Heliostat Field Layout CALculation).

HFLCAL is a tool for designing and optimizing heliostat fields for solar towers based on an annual performance calculation. The HFLCAL simulation is set up by specifying the heliostat configuration (size, shape and spacing between single heliostats), tower height, plant location, solar DNI, aperture shape and size, design time point and the incident power on the receiver. Then, the performance for a given amount of possible heliostat positions can be calculated and those with the best annual performance chosen. An optimization algorithm then allows the most cost-effective field layout to be identified. A detailed description of HFLCAL can be found in the literature [27,28]. Fig. 6 shows an exemplary heliostat field layout in HFLCAL.

The heliostat used for the field layout is a standard heliostat with a reflective area of 121 m^2.

The output from a HFLCAL simulation includes, amongst others:

- The number of heliostats and the total reflective area A_{helio} [m^2]
- Solar tower height H_{Tow} [m]
- Hourly field efficiency $\eta_{helio}(t)$ [%]

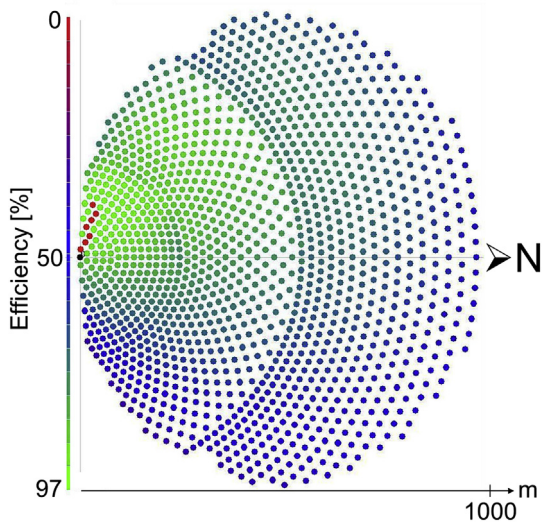

Fig. 6. Exemplary 72 MW heliostat field in HFLCAL: North is on the right, the black dot, center left, represents the solar tower.

The CPC efficiency is assumed to be 97% and is multiplied with the hourly field efficiency given by the HFLCAL simulation to yield the hourly field efficiency (including CPC) used for the further analysis. The field efficiency includes parameters such as the reflectivity of the mirrors, atmospheric attenuation, the cosine factor, the intercept factor, blocking and shading.

3.4. DNI and investigated plant location

The location investigated for this solar cement plant is Almeria in southern Spain. Almeria has proved to be a suitable location for solar thermal applications and the Plataforma Solar de Almeria is used as a testing facility for solar thermal components and power generation [29]. Furthermore, two cement plants are located around Almeria [30].

DNI data in hourly resolution for Almeria was obtained from Meyer and Schwandt [31,32]. Two data sets are used for the analysis, namely the P95 data for the base case and the P50 data set for investigation of a year with higher solar irradiation compared to the base case. P95 describes a data set, compared to which 95% of all years will have better annual solar irradiation and only 5% of years will have lower irradiation. Hence, this data is suitable for a conservative estimation of the potentials of solar cement plants. The P50 data, on the other hand, represents a “typical metrological year”, where the chance that one year's annual irradiation is higher or lower than the given data is 50%. Using this data for assessing the potential of a solar cement plant, which is in operation for many years, is hence more optimistic. With the given data set by Meyer and Schwandt, P50 and P95 represent the most optimistic and conservative approach, respectively. Both cases are compared in the following table (Table 2).

Table 2
Comparison of the DNI data [31].

Data Set	Annual DNI [kWh/m^2a]
P95 (base case)	2012
P50 (optimistic case)	2207

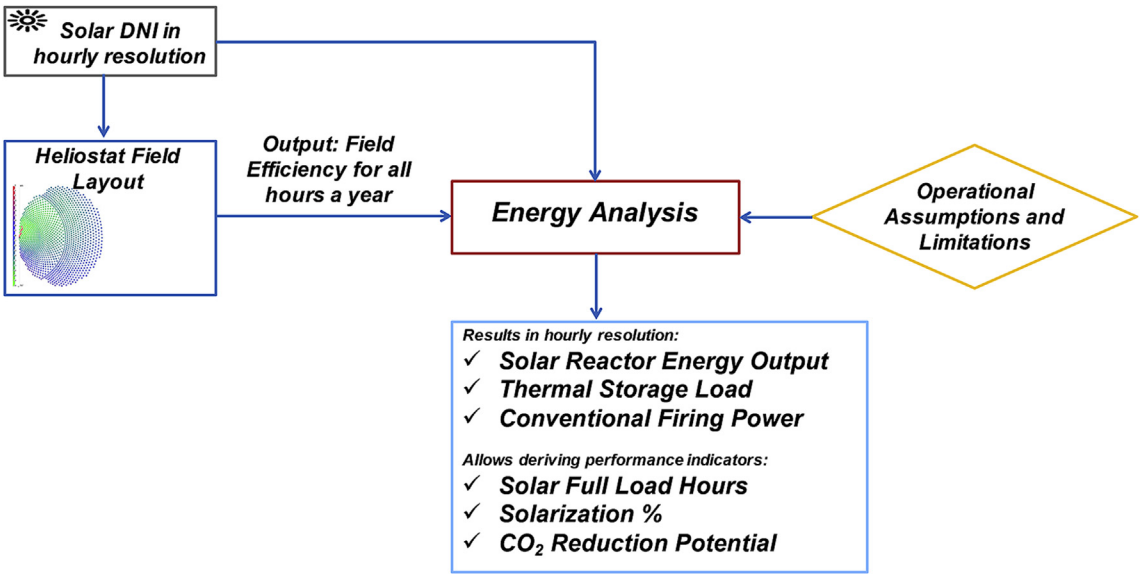

Fig. 7. Principle of energy analysis.

3.5. Energy analysis and plant operation

Fig. 7 shows the principle of energy analysis. Using HFLCAL, the field efficiency is calculated at an hourly resolution for all hours of a year. Together with the given solar DNI, the solar reactor's energy output, the thermal energy storage load and the conventional firing power is calculated at an hourly resolution. This allows determining the key performance indicators: solar full load hours, rate of process solarization and the CO_2 reduction potential.

Operation assumptions

In reality, a solar cement plant cannot be operated during all hours of solar irradiation. Several limitations and simplifications are therefore taken into consideration and implemented in the model:

Plant warm-up and minimum solar calciner load.

- The first hour of solar incident power on the reactor (after a minimum of 2 h without solar operation) is utilized for plant warm up. No reactions take place during warm-up.
- Below a minimum load of 20% of the calciner's design load, operation is not possible.

Maximum solar calciner load.

- The maximum load on the solar calciner is the design load. Additional solar incident power cannot be converted into calcined raw meal.

Thermal storage operation.

- Calcined meal surpassing the demand in the subsequent process is stored in the thermal storage system without losses at 100% thermal efficiency.
- In the case that the solar reactor cannot provide sufficient calcined meal for the subsequent process, the thermal storage provides for the deficit.

Conventional calciner operation in hybrid operation.

- In the case that the calcined raw meal from the solar calciner and thermal storage is not sufficient to supply the rotary kiln, the conventional calciner is operated.
- No minimum load restrictions exist for the conventional calciner.
- The efficiency for all load cases equals the efficiency of the conventional cement plant.

Operating time.

- As discussed before, the cement plant is operated 8000 h per year. For the sake of simplicity, it is assumed that the solar cement plant is operated during the first 8000 h of a year without interruption. Hence, during December the plant is not operated.

A detailed energy analysis model can be found in Appendix D.

3.6. Economic analysis and optimization

Economic and energy analysis are closely related. In particular, the thermal storage and heliostat field size have a large influence on the capacity factor, solarization rate and CO_2 emissions reduction. However, the larger the storage and heliostat field, the higher the costs. Hence, an optimization problem must be solved. This section gives an outline for the economic analysis.

The solar cement plant components (section 2) account for the capital costs. These are: heliostat field, solar tower, solar calciner, CPC, thermal storage, land and indirect costs [8,10,17].

The specific heliostat field, tower and thermal storage costs are taken from Dieckmann et al. [21]. The values used are cost projections for the year 2025.

The specific heliostat costs include site preparation, mirrors, drives, structure and foundation, as well as controls and installation. The tower costs are valid for tower heights of around 200 m [21], which is the case here. In cases where the solar cement plant consists of several solar fields, the tower costs are assumed to be 15% less compared to a single tower due to economies of scale.

Table 3
Definition of total annual costs, CO_2 avoidance, CO_2 avoidance costs and clinker costs.

Name	Symbol		Equation	
Total Annual Costs	$K_{an,tot}$	=	$K_{OPEX} + I_{CAPEX}{}^{*}a$	(Eq. 5)
CO_2 Avoidance (annual)	$m_{CO_2,av}$	=	$Q_{Fuel,save}c_{CO_2}$	(Eq. 6)
CO_2 Avoidance Costs	$k_{CO_2,av}$	=	$\frac{K_{an,tot}}{m_{CO_2,av}}$	(Eq. 7)
Clinker Costs	$k_{clinker}$	=	$k_{clinker,base} + \frac{K_{an,tot}}{m_{clinker,an}}$	(Eq. 8)

For the thermal storage costs, in accordance with González and Flamant [10], it is assumed that the storage medium costs are zero (as no additional storage medium is necessary). Only one storage tank is necessary (two tanks in state-of-the-art molten salt storage), and the pump and heat exchanger costs are doubled due to the high operating temperature. The heliostat field costs, tower costs and thermal storage costs are detailed and described in Appendix E.

CO_2 avoidance and clinker costs

To calculate the CO_2 avoidance and clinker costs, the annual CO2 avoidance and additional expenses due to the solar calcination have to be considered. These expenses are separated into the capital expenditure (CAPEX) and the operating expenditure (OPEX). The main difference is that the CAPEX is incurred once while the OPEX is an annually recurring cost. An overview of the defined costs is given in (Table 3).

The cost factors used for estimating the CPC costs, solar calciner costs and thermal storage system (TSS) costs are fairly uncertain compared to the other cost data. There is no experience in designing such systems for commercial plants yet. Other cost data, however, resemble existing commercial solar towers and are hence more reliable.

4. Results and discussion

The results for the solar calciner cement plant are presented in this section. Initially, section 4.1 considers whether large solar cement plants should be split into many small heliostat fields or if large single solar fields should instead be used. Section 4.2 then discusses how the thermal storage size and solar multiple influences the solarization rate and, hence, the CO_2 reduction. Different cases are holistically discussed and analyzed in section 4.3. A sensitivity analysis and conclusion are then given in section 4.4 and a comparison with the literature is carried out in 4.5. Unless otherwise stated, the DNI used here is P95 and the thermal calciner efficiency is 50%.

4.1. Single large solar field vs. several small fields

In general, the larger the heliostat field is, the lower the field's efficiency becomes. This is due to the fact, that the heliostats have a certain accuracy for reflecting the solar radiation onto the reactor. If the distance to the reactor increases, each additional heliostat becomes less effective, thermally and economically. Hence, from an efficiency perspective several small heliostat fields instead of a larger field are preferable. The number of heliostat fields was varied for a constant solar multiple of 2.5 and the capital costs compared, as shown in Fig. 8 and Table 4 (thermal storage size is assumed to be 12 h each).

The results show that while the heliostat field efficiency increases for an increasing number of small solar fields in comparison to larger fields, the CAPEX increases as well. The main reason for this is the increase in tower costs. Hence, the larger the solar field, the more economical the plant's CAPEX.

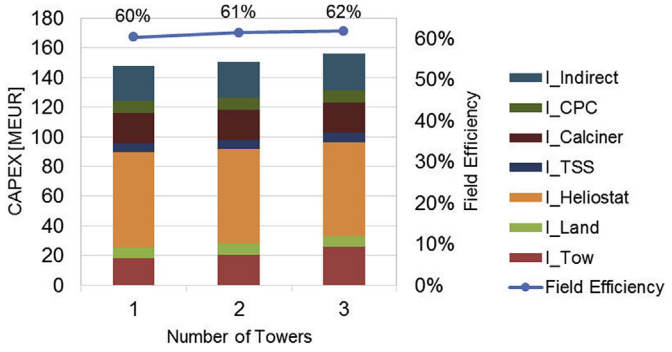

Fig. 8. CAPEX estimation for a variation in the number of solar fields for a 290 MW_{sol} solar plant.

Table 4
CAPEX estimation for a variation in the number of solar fields for a 290 MW_{sol} solar plant.

No. of Towers	$P_{Tow}^{sol,in}$ [MW_{sol}]	CAPEX [MEUR]	Field Efficiency [%]
1	290	148	60
2	145	150	61
3	97	156	62

As discussed above, a maximum solar tower size of 130 MW_{sol} is set as a boundary for realization. Hence, in the following cases, the largest solar field size below 130 MW_{sol} is discussed. In the above example, this would be the case for a three tower solar cement plant.

4.2. Thermal storage size, solar multiple and solarization rate

It is evident that the thermal storage size and solar multiple influence the solarization rate and, hence, the CO_2 reduction potential. Furthermore, a higher thermal storage size and solar multiple results in a higher CAPEX.

Fig. 9 shows the calciner solarization's dependence on the solar multiple and thermal storage size. It can be seen that with increasing thermal storage size, the achievable solarization ratio increases. Moreover, a maximum solarization ratio is reached. For an increasing solar multiple, this maximum is shifted towards an increasing thermal storage size. For example, a solar cement plant with SM = 1.5 and 2.0 reaches this maximum at a thermal storage size of around 4 h and 10 h, respectively. When the thermal storage size is increased beyond this point, the solarization does not change, as the solar field does not produce more excess energy that can be stored and utilized if irradiation is insufficient.

The CO_2 avoidance costs and clinker costs were calculated depending on the thermal storage size and solar multiple, too. The results are depicted in Fig. 10 and Fig. 11, respectively.

The costs of CO_2 avoidance decrease steadily from no storage to

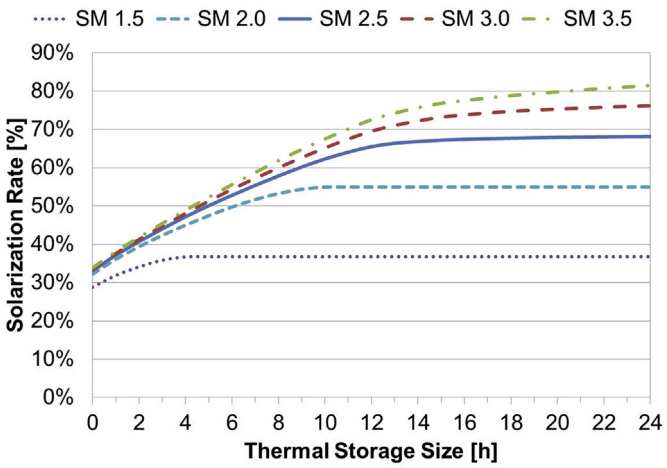

Fig. 9. Calciner solarization depending on thermal storage size and SM.

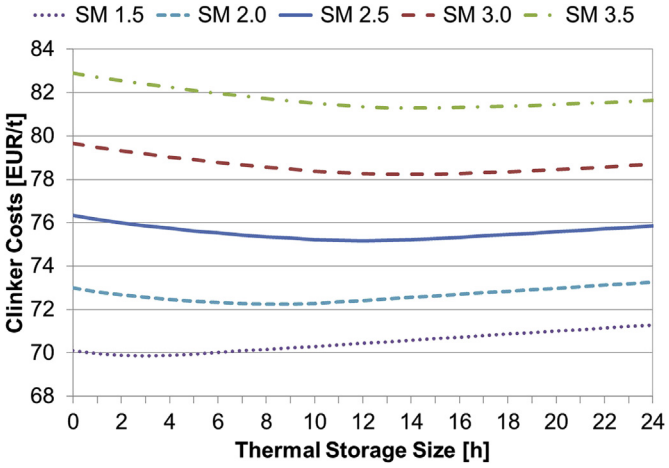

Fig. 11. Clinker costs depending on thermal storage size and solar multiple.

the point close to the maximum solarization rate, and then increase again. This first decrease is explained by the fact that the annual costs are allocated to a larger annual CO_2 avoidance, while the costs only increase marginally with the costs for thermal storage. After passing the minimum CO_2 avoidance costs, the costs increase again as an increase in thermal storage costs only shows little or no effect on the annual CO_2 avoidance. Therefore, an increasing cost sum is allocated to a (nearly) constant mass of CO_2 avoidance. This effect is especially visible for a solar multiple of 1.5 (Fig. 10), as here the total annual costs are lower than for the other cases and hence thermal storage costs have a higher impact on the overall costs. This leads to a stronger cost increase after the minimum avoidance costs, at around 4 h of storage.

In contrast, the clinker cost optimum is less prominent. The clinker costs remain nearly constant by varying less than 2 EUR for each solar multiple. The reason for this behavior is that the costs of the solar plant are allocated to the clinker production. For each SM, the annual costs are nearly constant, varying only by the thermal storage size and the cost savings by fuel substitution. Hence, the minimum clinker costs are slightly shifted to smaller storage sizes in comparison to the minimum CO_2 avoidance costs.

In general, the results show that the maximum achievable solarization rate is limited by the solar multiple. The larger the solar multiple, the larger the CO_2 avoidance. However, the solar multiple has a strong impact on the plant's economics. Fig. 9 shows that the solarization rate increases with a growing solar multiple, i.e., increasing the solar multiple from SM 1.5 to 2.5 leads to a doubled solarization rate, whereas the solarization rate between SM 2.5 and 3.5 only increases by a factor of 1.2. Hence, the tendency is slowed down. The more CO_2 that is avoided, the larger the costs for the solar cement plant.

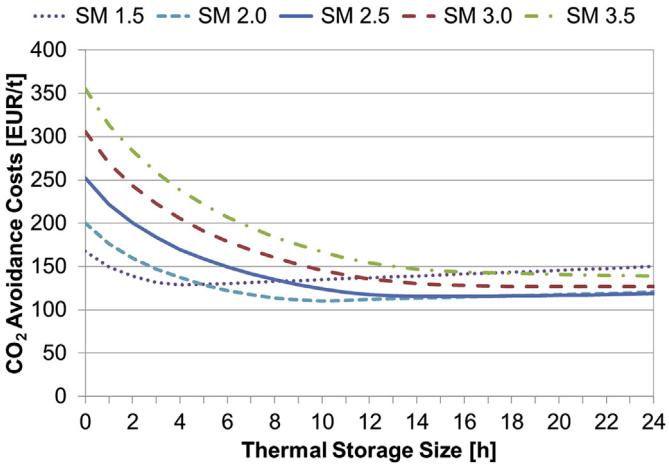

Fig. 10. CO_2 avoidance costs depending on thermal storage size and solar multiple.

4.3. Sensitivity analysis

In the following sections, a sensitivity analysis is conducted. Therefore, a base case is defined and five additional cases are investigated. Between each case, the reactor efficiency, DNI, solar multiple or a combination of these is varied. The technical and economic results are displayed in Table 5 and Table 6, respectively. The costs of CO_2 avoidance, clinker costs and solarization ratio are depicted in Table 6. The CAPEX pie charts for each case are shown in Appendix F. The optimum storage size is determined at the minimum clinker costs.

Base case

As a base case, the conservative DNI data set P95 (2012 kWh/m^2a) and a reactor efficiency of 50% is chosen. The solar multiple is set at 2.5, as this allows a solarization of 66% (13.8% overall CO_2 reduction) at the minimum clinker costs. The CO_2 avoidance costs are 118 EUR/t and the clinker costs 75 EUR/t. The CAPEX is 156 MEUR and the OPEX equals −0.95 MEUR (i.e., fuel savings are larger than the O&M costs), totaling 13.7 MEUR in annual costs.

Case 2: high reactor efficiency

In the second case, a higher reactor efficiency of 65% is investigated. All other assumptions remain the same compared to the base case. The optimum thermal storage size is found to be 12 h, allowing for a 65% solarization of the calciner (13.8% overall CO_2 reduction). The CO_2 avoidance costs are 87 EUR/t and the clinker costs, 72 EUR/t. The CAPEX is 125 MEUR and the OPEX -1.57 MEUR, totaling 10.1 MEUR in annual costs. The significant cost reduction of 26% compared to the base case mainly stems from a smaller required heliostat field due to the lower solar incident power required in a high efficiency calciner. The overall CO_2 reduction is smaller than in the base case. This derives from an increasing heliostat field size per tower, including a (marginally) reduced field efficiency.

Case 3: high DNI

In the third case, the influence of higher DNI (data set P50;

Table 5
Technical parameters of the investigated cases for a solar cement plant.

Name	Symbol	Base	Case 2	Case 3	Case 4	Case 5	Case 6	Unit
Assumed parameters								
DNI Data Set	/	P95	P95	P50	P50	P50	P50	/
Thermal Reactor Efficiency	η_{th}	50	65	50	65	65	65	%
Solar Multiple	SM	2.5	2.5	2.5	2.5	3.0	3.5	/
Calculated parameters								
Total Reflective Area of Heliostat Field	A_{helio}	70.4	53.9	62.8	48.5	57.4	67.6	ha
Field Efficiency	η_{field}	61.9	62.2	62.5	62.2	62.6	62.3	%
Tower Height	H_{Tow}	160	170	165	165	160	165	m
No. of Calciners per Tower	/	2	3	2	3	2	2	/
Calciner Thermal Power	$\dot{Q}_{SR,th}$	24	24	24	24	29	34	MW_{th}
No. of Towers	/	3	2	3	2	3	3	/
Solar Incident Power at Tower	$P_{Tow}^{sol,in}$	97	112	97	112	89	104	MW_{sol}
Thermal Storage Size	$Q_{TSS,design}$	697	697	697	697	813	871	MWh_{th}
	$t_{TSS,design}$	12	12	12	12	14	15	h
Total Land Area	A_{Land}	4.9	3.7	4.0	3.0	3.6	4.3	km^2
CO_2 Avoidance (annual)	$m_{CO_2,av}$	116	116	122	122	135	143	kt/a
Solar Full Load Hours	t_{sol}	5242	5237	5511	5513	6093	6450	h
Solarization Rate	SolR	66	65	69	69	76	81	%
Overall CO_2 reduction	CO_2R	13.8	13.8	14.5	14.5	16.1	17.0	%

Table 6
Economic results for the investigated cases of a solar cement plant.

Name	Symbol	Base	Case 2	Case 3	Case 4	Case 5	Case 6	Unit
Heliostat Field Costs	$I_{Heliostat}$	63.4	48.5	56.5	43.7	51.7	60.8	MEUR
Tower Costs	I_{Tow}	25.7	18.2	26.6	17.7	25.7	26.6	MEUR
Solar Calciner Costs	$I_{Calciner}$	20.3	20.3	20.3	20.3	22.1	23.8	MEUR
CPC Costs	I_{CPC}	8.43	6.47	8.43	6.47	7.79	9.07	MEUR
Thermal Storage System Costs	I_{TSS}	6.22	6.22	6.22	6.22	7.25	7.77	MEUR
Land Costs	I_{Land}	7.28	5.5	5.95	4.52	5.34	6.50	MEUR
Direct Costs	I_{Direct}	124	99.7	118	94.3	115	128	MEUR
Indirect Costs	$I_{Indirect}$	24.8	19.9	23.6	18.9	22.9	25.6	MEUR
CAPEX	/	156	125	148	118	143	160	MEUR
Annual O&M Costs	K_{OM}	3.12	2.50	2.95	2.35	2.86	3.20	MEUR
Annual Fuel Savings	$K_{Fuel,save}$	4.08	4.07	4.29	4.29	4.74	5.02	MEUR
OPEX	/	−0.95	−1.57	−1.34	−1.93	−1.88	−1.81	MEUR
Total Annual Costs	$K_{an,tot}$	13.7	10.1	12.5	9.09	11.5	13.2	MEUR
CO_2 Avoidance Costs	$k_{CO_2,av}$	118	87	102	74	85	92	EUR/t
Clinker Costs	$k_{clinker}$	75	72	74	71	73	75	EUR/t

2207 kWh/m^2a) is investigated. All other assumptions remain the same compared to the base case. The optimum thermal storage size was found to be 12 h, allowing for a 69% solarization of the calciner (14.5% overall CO_2 reduction). The CO_2 avoidance costs are 102 EUR/t and the clinker costs, 74 EUR/t. The CAPEX is 148 MEUR and the OPEX -1.34 MEUR, totaling 12.5 MEUR in annual costs. Hence, a location with a higher DNI allows for increasing the solarization rate and CO_2 reduction, while decreasing the costs compared to the base case. However, case 2 (high reactor efficiency) has a higher impact on the overall costs.

Case 4: high reactor efficiency and high DNI

Case 4 combines the higher reactor efficiency of 65% from case 2 with the higher DNI (P50) from case 3. The optimum thermal storage size was found to be 12 h, allowing for a 69% solarization of the calciner (14.5% overall CO_2 reduction). The CO_2 avoidance costs are 74 EUR/t and the clinker costs 71 EUR/t. The CAPEX is 118 MEUR and the OPEX equals −1.93 MEUR, totaling 9.09 MEUR in annual costs. Hence, the economic benefits of case 2 and 3 are combined, while the solarization rate of case 3 stays constant (analogous to the difference between the base case and case 2).

Case 5: solar multiple 3.0

In the following, two cases with a higher solar multiple of 3.0 and 3.5, and an optimistic reactor efficiency of 65% and DNI data set P50, are investigated.

For a solar multiple of 3.0, the optimum thermal storage size is found to be 14 h, allowing for 76% solarization of the calciner (16.1% overall CO_2 reduction). CO_2 avoidance costs are 85 EUR/t and clinker costs 73 EUR/t. The CAPEX is 143 MEUR and the OPEX is −1.88 MEUR, totaling 11.5 MEUR in annual costs.

Case 6: solar multiple 3.5

For a solar multiple of 3.5, the optimum thermal storage size (at minimum clinker costs) is found to be 15 h, allowing for 81% solarization of the calciner (17.0% overall CO_2 reduction). CO_2 avoidance costs are 92 EUR/t and clinker costs 75 EUR/t. The CAPEX is 160 MEUR and the OPEX is −1.81 MEUR, totaling 13.2 MEUR in annual costs.

A higher solar multiple, as discussed above, allows for increasing the solarization rate. However, at the same time, the costs significantly increase, too.

From the comparison, it can be obtained that by increasing the solar multiple, the solarization rate will be increased. The CO_2 avoidance cost is strongly influenced by the DNI set and SM, declining from 118 to 74 EUR/t, whereas the clinker cost (71–75 EUR/t) of each case is seldom affected by these factors. Fig. 12 summarizes the results.

4.4. Tornado analysis

In order to assess the sensitivity of the costs calculated to variations in the input parameters, a Tornado analysis was conducted

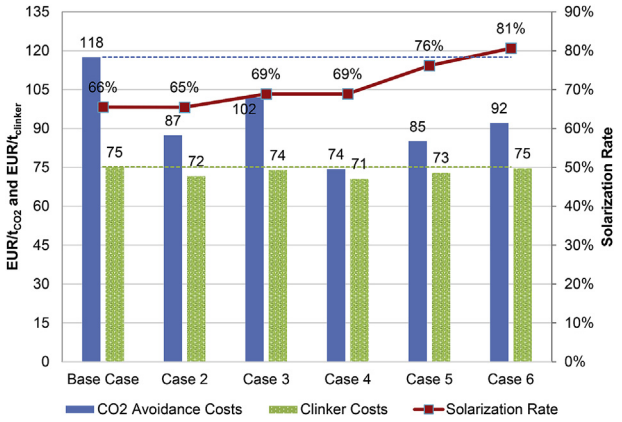

Fig. 12. CO_2 avoidance costs, clinker costs and solarization rate for the investigated cases.

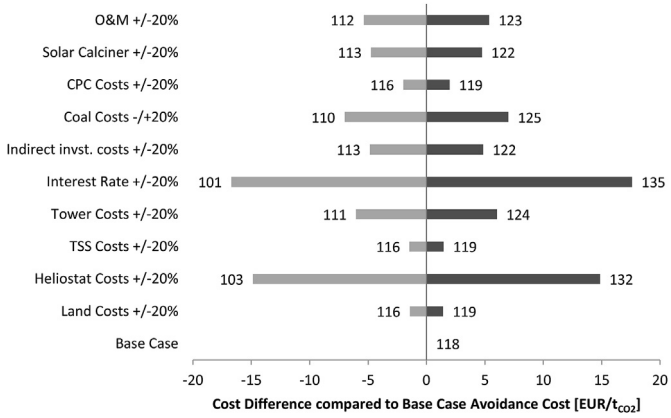

Fig. 13. Sensitivity analysis and CO_2 avoidance costs in the base case of the solar cement plant.

for the base case. The results are depicted in Fig. 13. Table 7 shows which parameters are varied in each case, as well as their value.

The major influences on the CO_2 avoidance costs are hence the interest rate and heliostat costs. The impact of the interest rate is significant, as the annual costs are mainly dominated by the depreciation of the CAPEX. The heliostat costs have a significant impact, as they represent the largest single cost factor, with around 40% of the overall CAPEX in all cases.

Interestingly, the costs for the solar calciner, the CPC costs and thermal storage system (TSS) costs show relatively little influence on the overall CO_2 avoidance costs. These three components are, however, those for which the cost estimations used here are the vaguest. The CPC costs were derived from the literature, where they were given for solar cement plants much smaller than the investigated plant. The solar calciner costs were derived from industrial rotary kilns and the TSS costs roughly derived from the literature, assuming that high temperature storage systems could be built at moderate costs. The sensitivity analysis shows that the economic results are relatively robust against variations of these three cost components. The capital costs are dominating compared to the variable costs. Therefore, the influence of the interest rate is correspondingly large.

4.5. Comparison with literature data

In the following, the obtained results are discussed and compared to the studies of Imhof and González and Flamant [10,17], as both investigated the large-scale solarization of industrial 3000 t/d cement plants. Alongside the base case, case 4 and case 6 of the paper are adopted for comparison. Two cases from González and Flamant's study [10], with a 70% solar reactor efficiency and 80% and 100% solarization are given in Table 8.

The present study's results show an increased cost compared to the cases found in the literature. A CAPEX of 156 MEUR, 118 MEUR and 160 MEUR in the base case, case 4 and case 6 face costs of 28 MEUR, 109 MEUR and 137 MEUR for Imhof [17], González and Flamant [10] at 80% and 100% solarization rate, respectively. The CO_2 avoidance costs in the work from Imhof [17] are estimated to be 50 EUR/t. In comparison, avoidance costs of 118, 74 and 94 EUR/t were calculated for the base case, case 4 and case 6, respectively.

Comparing the different component costs and technical parameters, following reasons for the differences can be named:

- Solar reactor thermal efficiency: Imhof assumes that reactor efficiency reaches 86%, while Gonzalez and Flamant assume a value of 70%. Both values are higher than the 50–65% considered in this case. A conservative approach was taken since such efficiencies were not shown up to now with industrial cement raw meal (see section 2). As was shown in section 4.3, the influence of the reactor efficiency on the costs is very high. An increase of the reactor efficiency of 15% points yields cost reductions of 26%. This shows the importance of further improving the reactor concepts and it has also to be added that scaling up of lab-scale reactors will also improve their efficiency.
- Optical field efficiency and net conversion factor: Gonzalez and Flamant estimate the optical field efficiency at 79%. HFLCAL simulations in the present work show that about 60% efficiency is realistic for heliostat fields of the size considered. Hence, the net conversion factor from solar incident power to thermal

Table 7
Sensitivity analysis: parameters and values varied.

Name	Parameter	Unit	Default Value	+20%	−20%
O&M	k_{OM}	%	2	2.4	1.6
Solar Calciner	k_{calcin}	EUR	405,665	486,798	324,532
CPC Costs (1)	k_{CPC}	EUR/MW	28,564	34,277	22,851
	I_{CPC}^{fix}	EUR	43,581	52,297	34,865
Coal price	k_{coal}	EUR/t	90	108	72
Indirect invst. costs	$k_{Indirect}$	%	20	24	16
Interest Rate	I	%	8	9.6	6.4
Tower Costs	k_{Tow}	EUR/m	63,106	75,727	50,485
TSS Costs	k_{TSS}	EUR/kWh$_{th}$	8.9	10.7	7.1
Heliostat Costs	k_{Helio}	EUR/m^2	90	108	72
Land Costs	k_{Land}	EUR/m^2	1.5	1.8	1.2

(1) For the CPC costs, both parameters $\boldsymbol{k_{CPC}}$ and $\boldsymbol{I_{CPC}^{fix}}$ are simultaneously varied.

Table 8
Comparison of obtained results with literature.

Study	Imhof 2000 [17]	Gonzalez and Flamant 2014 [10]		This paper		
		80% Solarization	100% Solarization	Base Case	Case 4	Case 6
Reference plant	3000 t/d	3000 t/d			3000 t/d	
Annual DNI [kWh/m^{2}a]	>2000 (not specified)	2,550[a]		2012	2207	2207
Solar component	calciner	calciner			calciner	
Thermal efficiency solar reactor [%]	86	70	70	50	65	65
Optical efficiency heliostat field [%]	/	79	79	62	62	62
Solarization Rate [%]	28	80	100	66	69	81
Annual CO_2 avoidance [%]	9	/	/	13.8	14.5	17.0
Solar power on kiln [MW_{th}]	/	228	285	290 [b]	224 [b]	313 [b]
Net conversion factor (solar to chemical) [%]	/	56	56	30	39	39
Solar Reactor costs [MEUR]	0.6	(6.6) [c]	(8.2) [c]	20.3	20.3	23.8
Tower costs [MEUR]	1.1 [d]	11.5 [d]	14.4 [d]	25.7	17.7	26.6
Heliostat costs [EUR/m^2]	133	133	133	90	90	90
Heliostat Field costs [MEUR]	19	55	68	63	44	61
Thermal Storage costs [MEUR]	/	13.2	16.6	6.2	6.2	7.8
CAPEX [MEUR]	22	109	137	156	118	160
CO_2 avoidance cost [EUR/t]	50	/	/	118	74	92

All cost data has been converted to EUR using an exchange ratio USD/EUR = 1.11 and CHF/EUR = 1.50.
[a] Own calculation from the monthly DNI data given in the study.
[b] Total solar power on kiln over all solar towers.
[c] Solar calciner costs are calculated using a formula derived from the CPC costs in Meier, Gremaud et al. [8].
[d] For preheater tower reinforcement.

energy only accounts for 30–39% in this paper, while Gonzalez and Flamant estimate a value of 56%.

- Solar reactor costs: In Imhof's case, solar reactor costs for a falling particle receiver were estimated at only 0.6 MEUR. Gonzalez and Flamant used cost data from Meier et al. [8] for the CPC to calculate the solar calciner costs. Hence, the solar reactor costs are lower than in this case. In the present study, solar reactor cost data was derived from industrially proven rotary kilns.
- Tower costs: Both previous studies assumed it to be sufficient to reinforce the cement plant's preheater tower and use it as a solar tower. However, this neglects that several solar towers might be necessary for supplying an industrial-scale cement plant. Hence, the tower costs cited in previous studies are lower.
- Solarization rate: Imhof's solarization rate of 28% seems reasonable compared to the cases assessed here without thermal storage (see Fig. 9). Gonzalez and Flamant's solarization rate of up to 100%, following the assumptions of the present study, seems difficult to achieve for the given costs. Fig. 9 shows that the achievable solarization rate difference decreases with increasing solar multiples. Hence, to achieve a solarization rate of 100%, a significantly large solar multiple – associated with higher costs – would be necessary. Another solution for 100% solarization would be to directly link the cement production to the DNI availability.

Together, the heliostat field costs, solar calciner costs and tower costs account for 70% of the CAPEX in the base case investigated. These costs were lower in previous studies, as high efficiencies for the reactors and heliostat fields were assumed. Also, reactor costs were lower and it was assumed that using existing preheater towers as solar towers is feasible.

5. CO_2 emission scenarios for Spain

In this section, we analyze which CO_2 reduction potential can be expected for Spain if conventional cement production is substituted by solar technology.

For Spain, cement demand projections are given for a base, low and high demand scenario by García-Gusano et al. [33]. In the high demand scenario, the cement demand reaches the cement consumption level prior to the financial crisis through 2050. In the base demand scenario, about half of the pre-crisis levels are reached by 2050. In the low demand scenario, the cement demand only rises marginally to less than 20 Mt until 2050. Here, it is assumed that demand can be equated to consumption.

The clinker-to-cement factor links clinker and cement production. It is assumed that all clinker necessary to satisfy the cement demand is produced in Spain. Clinker imports and exports are neglected. Furthermore, it is assumed that clinker production does not fall below today's level. Hence, from García-Gusano et al.'s cement demand scenarios, three clinker production scenarios are developed from today through 2050. Historical clinker production data is taken from Oficemen [34].

Fig. 14 shows the projected clinker production. In the base case, clinker production increases moderately to 23 Mt per year in 2050 from 18 Mt in 2016. In the low clinker production scenario, clinker production stagnates at the 2016 level of 18 Mt. In the high production scenario, clinker production reaches pre-crisis levels by 2040, further increasing through 2050, to 42 Mt clinker per year. In

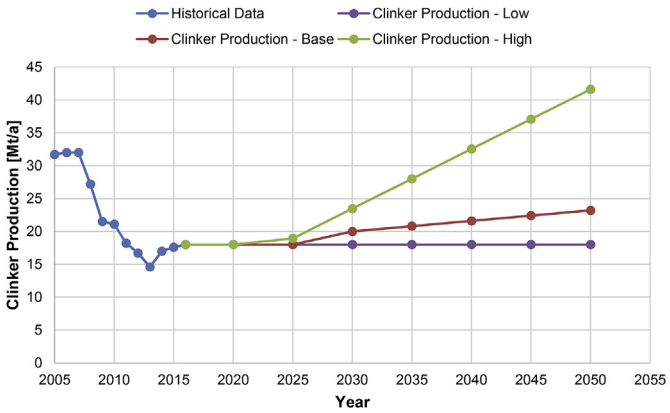

Fig. 14. Spanish clinker production projections until 2050; historical data from Oficemen [34].

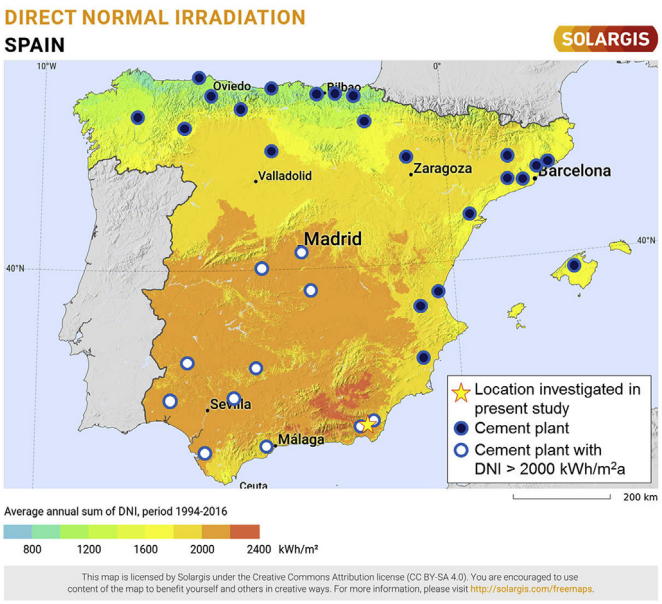

Fig. 15. Cement plant locations and DNI resource in Spain [34,35].

the high production scenario, new clinker production facilities must be built. In the other scenarios, existing clinker capacities are sufficient to meet national demand.

5.1. Suitable solar cement plant locations

All Spanish cement plants, their locations and clinker production capacities can be found in the yearbook of the Spanish Cement Association [34]. This data was combined with a map of the average DNI resources in Spain by Solargis [35], shown in Fig. 15. The map shows all cement plants and highlights those located at DNI values higher than 2000 kWh/m^{2}a.

Drawing from the clinker production data provided in Oficemen [34], the clinker production capacity in Spain for the 11 plants, with a minimum DNI of 2000 kWh/m^{2}a, is determined as 39 kt/d of a total of 99 kt/d clinker production capacity installed in 32 Spanish cement plants. If the average full load hours for all plants are assumed to equal 8000 h, then the annual clinker production capacity for all plants is determined as 33 Mt/a for all plants and 13 Mt/a for cement plants, with a minimum DNI of 2000 kWh/m^{2}a. Hence, 39% of all clinker production capacity could potentially be solarized. Table 9 summarizes the clinker production capacities and locations.

5.2. Emission scenarios for Spain: solar cement plants

Three emission scenarios are developed. For all scenarios, it is assumed that the solar calciner technology will be ready for commercial utilization by 2025:

- Base Scenario: 30% of all clinker in Spain is produced using the solar calciner technology through 2050. This assumes that nearly all of today's plants with a sufficiently high DNI are retrofitted/rebuilt as solar cement plants.
- Pessimistic Scenario: 15% of all clinker in Spain is produced using the solar calciner technology until 2050.
- Optimistic Scenario: 50% of all clinker in Spain is produced using the solar calciner technology until 2050.

Hence, in the base and pessimistic scenarios, the existing plant infrastructure would not need to be changed – plants at locations with high DNI could be retrofitted or new solar cement plants could be built at their locations. In the optimistic scenario, however, the distribution of clinker production in Spain would need to be changed and an increasing percentage of clinker would need to be produced in southern Spain in the future.

Today, specific CO_2 emissions in the Spanish cement industry average 829 $kg_{CO2}/t_{clinker}$ [34]. It is assumed that the base case CO_2 reduction is applied in all solarization scenarios, i.e., all solar cement plants show a solarization rate of 66% and 13.8% CO_2 reduction. Hence, the average specific emissions for all scenarios are calculated (Table 10). It is assumed that no other CO_2 emission reductions by other technologies are applied. The CO_2 emission scenarios show the impact of solarizing a fraction of Spanish cement plants in Spain on the overall CO_2 emissions. In the base case it is 4%, in the pessimistic case 2% and in the optimistic case up to 7% of the overall CO_2 emissions that could be saved in the respective scenarios.

To estimate the total CO_2 emissions in the respective scenarios, the future specific emissions for the three scenarios above are derived and combined with the clinker production scenarios. Fig. 16 shows the CO_2 emission scenarios for base, low and high clinker production. Table 11 shows the numeric results.

Table 9
Cement plants and clinker production capacity in Spain according to DNI resources [34,35].

DNI [kWh/a]	Daily Clinker Capacity [kt/d]	Annual Clinker Capacity [Mt/a]	Ratio [%]
>2000	39	13	39
Rest	60	20	61
Total	**99**	**33**	**100**

Table 10
CO_2 emission scenarios for solar cement plants in Spain.

Year	Base Scenario			Pessimistic Scenario			Optimistic Scenario		
	Solar Plants	Specific Emissions		Solar Plants	Specific Emissions		Solar Plants	Specific Emissions	
		[$kg_{CO2}/t_{clinker}$]	%		[$kg_{CO2}/t_{clinker}$]	%		[$kg_{CO2}/t_{clinker}$]	%
2016	0%	829	0	0%	829	0	0%	829	0
2020	0%	829	0	0%	829	0	0%	829	0
2030	6%	822	−1	3%	826	0	10%	818	−1
2040	18%	808	−2	9%	819	−1	30%	795	−4
2050	30%	795	−4	15%	812	−2	50%	772	−7

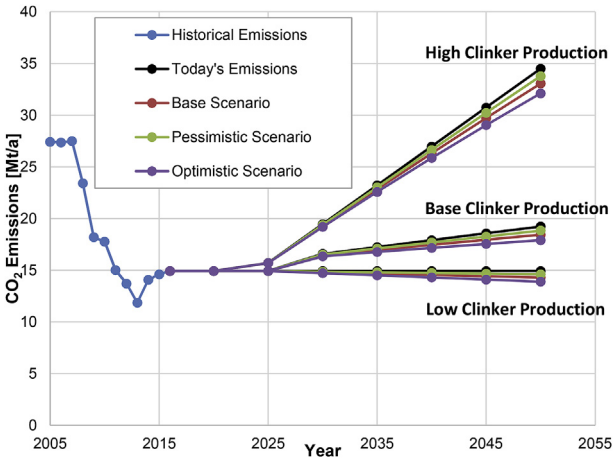

Fig. 16. Solar cement plant: CO_2 emission projections (historical data from Oficemen [34]).

The effect of solarizing only a fraction of Spanish cement plants, by replacing the fossil fuel in the calcination with solar energy, against the overall CO_2 emissions is limited. In the base clinker production scenario, a base case solarization of cement plants in Spain would contribute to a CO_2 reduction of 800 kt/a by 2050, 400 kt/a in the pessimistic scenario and 1.3 Mt/a in the optimistic scenario. In a low demand scenario, the CO_2 reduction amounts to 600 kt/a, 300 kt/a and 1 Mt/a, respectively. In the high demand scenario, in the base case of 1.4 Mt/a, in the pessimistic case of 700 kt/a and in the optimistic case, 2.4 Mt/a of CO_2 are reduced by 2050. In relation to the overall emissions for today's emission factor of 19 Mt/a, 15 Mt/a and 35 Mt/a, these reductions are comparatively low. This clearly shows, that aside from a solarization of the process additional sequestration of the reaction gas during the calcination has to be considered for a bigger impact. As was discussed in section 3.2, the impact could be increased by a factor of four if a controlled sequestration of the CO_2 in the solar reactor is implemented. Furthermore it was shown in section 4.3 that improving the reactor efficiency by only 15% points reduces the CO_2 avoidance costs already by 26%.

6. Conclusion

This paper presented a detailed analysis to explore solar thermal calciner technology in the cement industry. The potential for reducing the cement industry's CO_2 emissions is economically quantified. Furthermore, CO_2 emission projections for the clinker producing industry and emission reduction potentials are derived for Spain.

For solar cement plants, it is shown that the solar multiple and thermal storage size are the determining factors for the solarization rate, i.e., the possible CO_2 avoidance. The maximum CO_2 avoidance rate, equalling a 100% solarization of the calciner, is 21% in comparison to the overall cement plant emissions. The higher the solar multiple, the higher the CO_2 avoidance costs. However, in order to reach a 100% solarization, the solar multiple grows nonlinearly, making investment at a very high solarization rate unreasonable unless the cement production is directly linked to the available DNI. Hence, in the base case (SM = 2.5, reactor efficiency 50% and low DNI) the optimum solarization rate is 66%, i.e., 14% CO_2 avoidance, with avoidance costs of 118 EUR/t and clinker costs of 75 EUR/t. For cases 2 to 4, the reactor efficiency, DNI and both values are varied. The results show that increasing the reactor efficiency has a very strong impact on the CO_2 avoidance costs (87 EUR/t in case 2), as does an increasing DNI (102 EUR/t in case 3). An increase in the reactor efficiency by 15% points leads to a cost reduction of 26%. The combination of a high DNI and high reactor efficiency in case 4 results in CO_2 avoidance costs of 74 EUR/t, a cost reduction of 37% compared to the base case. While for both the base case and case 2 the CO_2 avoidance rate equals 14%, CO_2 avoidance increases to 15% with a higher DNI in cases 3 and 4. For cases 5 and 6, the solar multiple increases to 3.0 and 3.5, respectively, while retaining case 4's high DNI and reactor efficiency. For these cases, a CO_2 avoidance rate of 16% and 17% at avoidance costs of 85 EUR/t and 92 EUR/t are achieved.

An analysis of cement plant locations in Spain shows that 39% of plants today are located in areas with sufficient solar irradiation, which makes the application of solar calciner technology feasible. For the base case, an adaptation of 30% for all cement plants in Spain is assumed (with a CO_2 avoidance of 13.8% per plant, as in the respective base case). CO_2 emission reductions are achievable from 0.6 to 1.4 Mt/a by 2050, depending on the clinker produced. This amounts to CO_2 avoidance for the entire Spanish cement industry

Table 11
CO_2 emission projections for solar cement plants in Spain.

Year	Today's Emissions	Base Scenario		Pessimistic Scenario		Optimistic Scenario	
	Emissions [Mt/a]	Emissions [Mt/a]	Emissions Avoided [Mt/a]	Emissions [Mt/a]	Emissions Avoided [Mt/a]	Emissions [Mt/a]	Emissions Avoided [Mt/a]
Base Clinker production							
2016	15	15	0.0	15	0.0	15	0.0
2020	15	15	0.0	15	0.0	15	0.0
2030	17	16	−0.1	17	−0.1	16	−0.2
2040	18	17	−0.4	18	−0.2	17	−0.7
2050	19	18	−0.8	19	−0.4	18	−1.3
Low Clinker Production							
2016	15	15	0.0	15	0.0	15	0.0
2020	15	15	0.0	15	0.0	15	0.0
2030	15	15	−0.1	15	−0.1	15	−0.2
2040	15	15	−0.4	15	−0.2	14	−0.6
2050	15	14	−0.6	15	−0.3	14	−1.0
High Clinker Production							
2016	15	15	0.0	15	0.0	15	0.0
2020	15	15	0.0	15	0.0	15	0.0
2030	19	19	−0.2	19	−0.1	19	−0.3
2040	27	26	−0.7	27	−0.3	26	−1.1
2050	35	33	−1.4	34	−0.7	32	−2.4

of 4%. If 50% of plants adopt solar calciner technology by 2050, emission reductions would total 7% (in the optimistic case) and 2% in the pessimistic case (15% adaptation). One way to significantly improve this would be to implement a controlled sequestration of the CO_2 in the solar calciner. This would result in emission reductions from 8 to 28%.

Acknowledgements

This work was supported by the Helmholtz Association under the Joint Initiative "EnergySystem 2050 – A Contribution of the Research Field Energy" and has received funding from the European Union's Horizon 2020 research and innovation programme under grant agreement No. 654663 (SOLPART project).

Nomenclature

Latin and Greek Symbols

a	Annuity
A	Area (m^2)
C	Concentration factor
c_{CO_2}	Specific CO_2 emissions factor per unit of heat content
c_p	Specific heat (J/kg K)
CO_2R	Overall CO_2 reduction rate (%)
f_M	Material factor
f_P	Pressure factor
f_T	Temperature factor
ΔH	Enthalpy
H	Height (m)
I	Investment costs (EUR)
I_{ap}	Irradiation on Aperture (kW/m^2)
k	Specific costs per unit (EUR/unit)
K	Annual costs (EUR/a)
m	Mass (kg)
$\dot{m}$	Mass Flow (kg/s)
P	Capacity size (flux) of equipment (Eq. (24) and Eq. (25)) (W)
$P_{Tow}^{sol,in}$	Solar incident power at tower (W)
Q	Heat energy (J)
$\dot{Q}$	Heat flux (W)
SolR	Calciner process solarization (%)
T	Time (s)
T	Temperature (K)
X^{dc}	Calcination degree (%)
Y	Mass fraction (%)
η	Efficiency (%)

Subscripts

an	Annual
calcin	(Pre-)Calcination
CO_2,av	CO_2 avoided
Conv	Conventiona
el	Electric
g	Gas
helio	Heliostat
in	Incident/input
kiln	Rotary kiln
red	Reduction
rm	Raw meal
sol	Solar
SR	Solar reactor/calciner
th	Thermal
tot	Total
Tow	Tower

Abbreviations

BD	Beam down
CAPEX	Capital expenditures
CPC	Compound parabolic concentrator
CSP	Concentrated solar power
DNI	Direct Normal Irradiation
HFLCAL	Heliostat Field Layout Calculation
LHV	Lower heating value
O&M	Operation and maintenance
OPEX	Operational expenditures
SM	Solar multiple
TSS	Thermal storage system
TT	Top of tower

Appendix

A. Heat Balance Calculation in a Solar Calciner

A heat balance around the solar calciner yields:

$$\dot{\boldsymbol{Q}}_{\mathbf{rm,heat}} + \dot{\boldsymbol{Q}}_{\mathbf{calcin}} = \dot{\boldsymbol{Q}}_{\mathbf{TA}} + \dot{\boldsymbol{Q}}_{\mathbf{KG}} + \dot{\boldsymbol{Q}}_{\mathbf{SR,th}} \tag{9}$$

where $\dot{Q}_{TA}$ and $\dot{Q}_{KG}$ are the heat input by the tertiary air (TA) and kiln gas (KG), respectively. $\dot{Q}_{calcin}$ is the energy required for the calcination and $\dot{Q}_{rm,heat}$ the energy required for heating up the raw meal from the calciner inlet temperature to calcination temperature. $\dot{Q}_{SR,th}$ is the solar calciner's thermal energy input from which the solar incident power $\dot{Q}_{sol,in}$ is calculated as:

$$\dot{\boldsymbol{Q}}_{\mathbf{sol,in}} = \frac{\dot{\boldsymbol{Q}}_{\mathbf{SR,th}}}{\boldsymbol{\eta}_{\mathbf{th}}} \tag{10}$$

where η_{th} is the thermal efficiency of the solar calciner.

It is assumed that both gas streams mix ideally and leave the solar calciner at a common temperature $T_{out,g}$. The heat influx by the gas streams (with mass flow $\dot{m}_{TA/KG}$, specific heat $c_{p,TA/KG}$ and inlet temperature $T_{in,TA/KG}$) is calculated as:

$$\dot{\boldsymbol{Q}}_{\mathbf{TA/KG}} = \dot{\boldsymbol{m}}_{\mathbf{TA/KG}} \boldsymbol{c}_{\mathbf{p,TA/KG}} \left(\boldsymbol{T}_{\mathbf{in,TA/KG}} - \boldsymbol{T}_{\mathbf{out,g}} \right) \tag{11}$$

The heat required for heating the raw meal mass from the inlet temperature to the calcination temperature $\dot{Q}_{rm,heat}$ is:

$$\dot{\boldsymbol{Q}}_{\mathbf{rm,heat}} = \dot{\boldsymbol{m}}_{\mathbf{rm}} \boldsymbol{c}_{\mathbf{p,rm}} \left(\boldsymbol{T}_{\mathbf{calcin}} - \boldsymbol{T}_{\mathbf{in,rm}} \right) \tag{12}$$

where $c_{p,rm}$ is the specific heat of the raw meal and T_{calcin} and $T_{in,rm}$ the calcination temperature and the raw meal temperature at the inlet, respectively.

$\dot{Q}_{calcin}$ is calculated from the mass flow rate of the raw meal at the inlet of the solar calciner $\dot{m}_{rm}$ multiplied by the relative calcium oxide content $Y_{rm,CaO}$ and the specific calcination energy referred to CaO ΔH_{CaO}^{calcin} [10].

$$\dot{\boldsymbol{Q}}_{\mathbf{calcin}} = \dot{\boldsymbol{m}}_{\mathbf{rm}} \boldsymbol{Y}_{\mathbf{rm,CaO}} \left(\boldsymbol{X}_{\mathbf{out}}^{\mathbf{dc}} - \boldsymbol{X}_{\mathbf{in}}^{\mathbf{dc}} \right) \Delta \boldsymbol{H}_{\mathbf{CaO}}^{\mathbf{calcin}}, \tag{13}$$

where $X_{in/out}^{dc}$ is the degree of calcination at the solar reactor's inlet and outlet, respectively.

These equations now allow the layout of the solar cement plant process. The data as well as additional equations used for calculating the raw meal mass flow and specific heat capacities used for the calculation are given in Appendix B and C.

The thermal energy input to the solar calciner is determined to

be 58 MW_{th} for continuous operation. Assuming a reactor efficiency η_{th} of 50%, the necessary solar incident power equates to 116 MW_{sol}. Table 12 summarizes the results derived from the heat balance.

Table 12
Heat balance results.

Variable	Value	Unit
$\dot{Q}_{TA}$	5.4	MW_{th}
$\dot{Q}_{KG}$	4.1	MW_{th}
$\dot{Q}_{calcin}$	58.8	MW_{th}
$\dot{Q}_{rm,heat}$	8.8	MW_{th}
$\dot{Q}_{SR,th}$	58.1	MW_{th}
$\dot{Q}_{sol,in}$	116 ($\eta_{th} = 0.5$)	MW_{sol}

B. Heat and Mass Balance – Stream Data

$$c_{p,exit\ gas}\left[\frac{kJ}{kg\ K}\right] = 0.96 + 0.000209 \cdot t \quad \text{(Eq. 16)}$$

$$c_{p,CO_2}\left[\frac{kJ}{kg\ K}\right] = 0.80 + 0.000461 \cdot t \quad \text{(Eq. 17)}$$

where t is the temperature in °C. For the sake of simplicity, the average temperature between the inlet and outlet for each stream was used in the calculation.

D. Energy Analysis Model

The analysis is done via analytical equations and balances, explained in this section. The formulated equations were solved in EXCEL. Plant operation is briefly explained for a solar multiple of SM > 1 over the time of one day and schematically depicted in Fig. 17. During the first and last hour(s) of solar irradiation, the solar power is not sufficient to power the solar calciner; all calcined meal is provided by the thermal storage and/or the conventional firing system. However, the existing solar irradiation is used for solar reactor warm up. When the solar power reaches 20% of the reactor design point, the solar calciner begins operation. The deficit between the produced calcined meal and the design point is again supplied from the storage or fossil calciner. When the solar reactor reaches the process design point, all calcined meal is directly fed to the subsequent process. In the case of a solar multiple >1, the solar reactor generates excess meal, which is stored in the thermal storage. However, the reactor cannot operate at a higher load than the design point load. Hence, energy exceeding the design point is not exploited.(see Fig. 18)

Table 13
Data for heat and mass balance calculation solar calciner.

Parameter	Description	Value	Unit	Source
$\dot{m}_{TA}$	Tertiary air mass flow	26.2	kg/s	[25]
$T_{in,TA}$	Temperature of tertiary air at inlet	1050	°C	[25]
$T_{out,g}$	Gas temperature at calciner exit	871	°C	[25]
$\dot{m}_{KG}$	Kiln gas mass flow	17.1	kg/s	[25]
$T_{in,KG}$	Kiln gas temperature at inlet	1078	°C	[25]
X^{dc}_{out}	Degree of calcination at calciner exit	0.95	–	[26]
X^{dc}_{in}	Degree of calcination at calciner inlet	0.18	–	[26]
ΔH^{calcin}_{CaO}	Calcination enthalpy at 900 °C, 1atm	3182	kJ/kg	[10]
$Y_{rm,CaO}$	Mass fraction of CaO in raw meal	0.4322	–	[26]
$\dot{m}_{clinker}$	Clinker mass flow	34.72	kg/s	[26]
$\dot{m}_{rm}/\dot{m}_{clinker}$	Raw-meal-to-clinker factor	1.6	–	[26]
T_{calcin}	Calcination temperature	900	°C	[26]
$T_{in,rm}$	Raw meal temperature at inlet	759	°C	[25]
$\dot{m}_{coal,calcin}$	Coal mass flow into calciner	2.4	kg/s	[25]
LHV_{coal}	Lower heating value of coal	27,150	kJ/kg	[25]
c_{CO_2}	Specific CO_2 emissions for Coal	$9.465 \cdot 10^{-5}$	kg/kJ	[26]
Y_{rm,CO_2}	Mass fraction of CO_2 in the raw meal	0.3474	–	[26]
$\dot{m}_{coal,kiln}$	Coal mass flow into clinkering kiln	1.469	kg/s	[26]

C. Approximation of Specific Heat Capacities

According to Labahn and Kohlhaas [36], the specific heat capacity of all flue gas and mass components can be calculated as follows:

$$c_{p,clinker}\left[\frac{kJ}{kg\ K}\right] = 0.8 + 0.000297 \cdot t \quad \text{(Eq. 14)}$$

$$c_{p,rm}\left[\frac{kJ}{kg\ K}\right] = 0.88 + 0.000293 \cdot t \quad \text{(Eq. 15)}$$

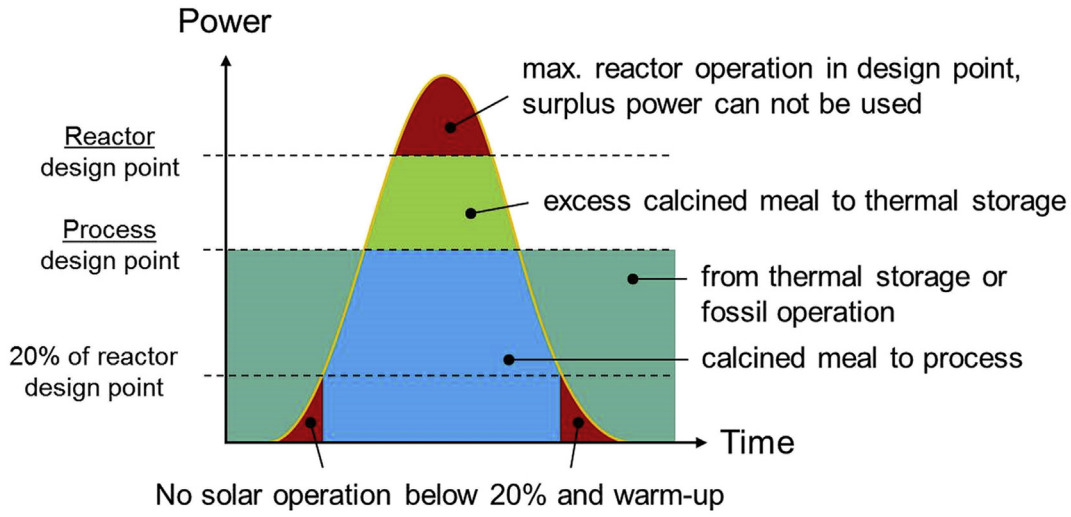

Fig. 17. Solar cement plant operation during daytime for a plant with a solar multiple SM > 1 (schematic).

The solar incident power is determined from the heliostat field area A_{helio}, the field efficiency $\eta_{helio}(t)$ and solar DNI(t) in hourly resolution:

$$\dot{\boldsymbol{Q}}_{\mathbf{sol,in}}(\boldsymbol{t}) = \boldsymbol{A}_{\mathbf{helio}}\boldsymbol{\eta}_{\mathbf{helio}}(\boldsymbol{t})\mathbf{DNI}(\boldsymbol{t}) \tag{18}$$

Together with the solar calciner's thermal efficiency and taking the above limitations into consideration, the calciner's thermal energy output is determined:

$$\dot{\boldsymbol{Q}}_{\mathbf{SR,th}}(\boldsymbol{t}) = \boldsymbol{\eta}_{\mathbf{th}}\dot{\boldsymbol{Q}}_{\mathbf{sol,in}}(\boldsymbol{t}) \tag{19}$$

As discussed above, several cases now exist:

- The raw meal production is larger or equal to the raw meal demand from the rotary kiln $\dot{Q}_{SR,th}(t) \geq \dot{Q}_{demand}$, then:
  - $\dot{Q}_{demand}$ is directly fed to the subsequent process (i.e., the sintering rotary kiln),
  - As long as the thermal storage has not reached its design load $Q_{TSS} < Q_{TSS,design}$, the raw meal excess is fed to the thermal storage:

$$\dot{\boldsymbol{Q}}_{\mathbf{TSS,in}}(\boldsymbol{t}) = \dot{\boldsymbol{Q}}_{\mathbf{SR,th}}(\boldsymbol{t}) - \dot{\boldsymbol{Q}}_{\mathbf{demand}} \tag{20}$$

$$\dot{\boldsymbol{Q}}_{\mathbf{TSS,out}}(\boldsymbol{t}) = \dot{\boldsymbol{Q}}_{\mathbf{demand}} - \dot{\boldsymbol{Q}}_{\mathbf{SR,th}}(\boldsymbol{t}) \tag{21}$$

$$\dot{\boldsymbol{Q}}_{\mathbf{conv}}(\boldsymbol{t}) = \dot{\boldsymbol{Q}}_{\mathbf{demand}} - \dot{\boldsymbol{Q}}_{\mathbf{SR,th}}(\boldsymbol{t}) - \dot{\boldsymbol{Q}}_{\mathbf{TSS,out}}(\boldsymbol{t}) \tag{22}$$

  - However, if the thermal storage is full $Q_{TSS} = Q_{TSS,design}$, then no excess raw meal is produced in the calciner (i.e., operation at partial load).
- The raw meal production is less than the raw meal demand from the subsequent process $\dot{Q}_{SR,th}(t) < \dot{Q}_{demand}$, therefore:
  - The difference between the demand and calciner output is fed by the thermal storage, as long as the thermal storage is not empty $Q_{TSS} > 0$:
  - If the thermal storage is empty $Q_{TSS} = 0$, or the stored meal is not sufficient to satisfy the demand $\dot{Q}_{TSS,out}(t) < \dot{Q}_{demand} - \dot{Q}_{SR,th}(t)$, then the conventional, fossil-fired operation makes up the difference:

The heat supplied by conventional firing $\dot{Q}_{conv}(t)$ is summed up over all hours per year $\sum_{t=0}^{8000} \dot{Q}_{conv}$. This allows the key performance indicators of the energy analysis to be determined:

Full load hours in fossil operation: $$\boldsymbol{t}_{\mathbf{fossil}} = \frac{\sum_{t=0}^{8000}\dot{\boldsymbol{Q}}_{\mathbf{conv}}}{\dot{\boldsymbol{Q}}_{\mathbf{conv,full}}} \tag{23}$$

Full load hours in solar operation: $$\boldsymbol{t}_{\mathbf{sol}} = 8000\ \mathbf{h} - \boldsymbol{t}_{\mathbf{fossil}} \tag{24}$$

Calciner process solarization (SolR): $$\mathbf{SolR} = \frac{\boldsymbol{t}_{\mathbf{sol}}}{8000\ \mathbf{h}} \tag{25}$$

Annual Fuel Savings $$\boldsymbol{Q}_{\mathbf{Fuel,save}} = \dot{\boldsymbol{Q}}_{\mathbf{conv,full}}\boldsymbol{t}_{\mathbf{sol}} \tag{26}$$

- Overall CO_2 reduction (CO_2R) for the cement process: $CO_2R = SolR \cdot 21\%$, where 21% is the maximum CO_2R determined in section 3.2.

The thermal storage size $Q_{TSS,design}$ is calculated as the product of design storage hours t_{TSS} and the solar reactors thermal energy throughput $\dot{Q}_{SR,th}$:

$$\boldsymbol{Q}_{\mathbf{TSS,design}} = \dot{\boldsymbol{Q}}_{\mathbf{SR,th}}\boldsymbol{t}_{\mathbf{TSS}} \tag{27}$$

The storage size is determined by means of optimization.

The conventional firing full load $\dot{Q}_{conv,full}$ is determined from the reference plant as:

$$\dot{\boldsymbol{Q}}_{\mathbf{conv,full}} = \dot{\boldsymbol{m}}_{\mathbf{coal,calcin}}\boldsymbol{LHV}_{\mathbf{coal}} = 65.2\ \mathbf{MW_{th}} \tag{28}$$

which is equal to an efficiency of $\eta_{conv} = 89\%$ in comparison to the solar calciner.

E. Heliostat Field, Tower and Thermal Storage Costs

Table 14 shows the cost components of the thermal storage system. In accordance with González and Flamant [10], it is assumed that the storage medium costs are zero (as no additional storage medium is necessary). Only one storage tank is necessary

and the pump and heat exchanger costs are doubled due to the high operating temperature.

Table 14
Costs for the thermal storage system (TSS), molten salt storage costs from literature [21].

Component	Costs Molten Salt Storage	Costs Solar Calcined Meal Storage	Unit
Storage Medium	8.5	0.0	EUR/kWh$_{th}$
Tanks	8.2	4.1	EUR/kWh$_{th}$
Pumps and Heat Exchangers	1.6	3.2	EUR/kWh$_{th}$
Balance of Plant Storage	1.6	1.6	EUR/kWh$_{th}$
Total k_{TSS}	**19.8**	**8.9**	EUR/kWh$_{th}$

Costs are adjusted to EUR using an exchange rate of USD/EUR = 1.11.

Solar calciner costs

Up until now, only lab-scale solar calciners have been built. Hence, no reliable cost data exists. However, it is likely that solar rotary kiln calciners will resemble the (fossil fuel-fired) rotary kilns used in heavy industry. For waste incinerator rotary kilns, cost data was derived from Garrett [37]. It is assumed that those costs could be reduced by 30% for solar calciners, as the firing equipment and associated equipment are not necessary.

CPC costs

CPC costs are derived from the literature [9,10] on a MW solar incident basis.

Tables 15 and 16 show the equations and values used in the CAPEX calculation. The OPEX consists of O&M costs and the savings associated with a reduction in fuel costs in comparison to the conventional cement plant. OPEX calculation equations are given in Table 17 and Table 18. All other cost factors for equipment or operations, such as transportation of raw meal and calcined meal to and from the solar tower, additional electricity costs etc., are neglected.

Table 15
Solar cement plant CAPEX cost factors and computation.

Name	Symbol		Equation		Source
Heliostat Field Costs	I_{Helio}	=	$k_{Helio}A_{helio}$	(Eq. 29)	/
Tower Costs	I_{Tow}	=	$k_{Tow}H_{Tow}$	(Eq. 30)	/
Solar Calciner Costs	$I_{Calciner}$	=	$k_{calcin}\left(\frac{\dot{Q}_{SR,th}}{P^{ref}_{calcin}}\right)^{0.48}$	(Eq. 31)	[37]
CPC Costs	I_{CPC}	=	$k_{CPC}P^{sol.in}_{Tow} + I^{fix}_{CPC}$	(Eq. 32)	[9,10]
Thermal Storage System Costs	I_{TSS}	=	$k_{TSS}Q_{TSS,design}$	(Eq. 33)	/
Land Costs	I_{Land}	=	$k_{Land}A_{Land}$	(Eq. 34)	/
Direct Costs	I_{Direct}	=	$I_{Helio} + I_{Tow} + I_{Calciner} + I_{CPC} + I_{TSS}$	(Eq. 35)	/
Indirect Costs	$I_{Indirect}$	=	$k_{Indirect}I_{Direct}$	(Eq. 36)	/
CAPEX	CAPEX	=	$I_{Direct} + I_{Indirect} + I_{Land}$	(Eq. 37)	/

Table 16
Specific investment costs and parameters for solar cement plant CAPEX computation.

Name	Symbol	Value	Unit	Source
Specific Heliostat Field Costs	k_{Helio}	90	EUR/m^2	[21]
Specific Tower Costs(1)	k_{Tow}	63,106 (53,640) (1)	EUR/m	[21]
Specific Solar Calciner Costs	k_{calcin}	405,665	EUR	[37]
Reference Calciner Thermal Power	P^{ref}_{calcin}	293	kW$_{th}$	[37]
Specific CPC costs	k_{CPC}	28,564	EUR/MW	[9]
Solar Incident Power at Tower	$P^{sol.in}_{Tow}$	$\frac{\dot{Q}_{sol.in}}{\text{No. of Towers}}$	MW$_{sol}$	/
Fixed Costs CPC	I^{fix}_{CPC}	43,581	EUR	[9]
Specific TSS Costs	k_{TSS}	8.9	EUR/kWh$_{th}$	[10,21]
Thermal Storage Size	Q_{TSS}	s. section 3.5	kWh$_{th}$	/
Specific Land Costs	k_{Land}	1.5	EUR/m^2	Assumption
Specific Indirect Costs	$k_{Indirect}$	20	%	Assumption

All cost data is adjusted to 2016 EUR using the corresponding Chemical Engineering's Plant Cost Index (CEPCI); USD/EUR = 1.11.
(1) For two and more solar towers, the costs are assumed to be reduced by 15%.

Table 17
Solar cement plant OPEX cost factors and computation.

Name	Symbol		Equation	
Annual O&M Costs	K_{OM}	=	$k_{OM}I_{Tot}$	(Eq. 38)
Annual Fuel Savings	$K_{Fuel,save}$	=	$Q_{Fuel,save}k_{coal}$	(Eq. 39)
OPEX	OPEX	=	$K_{OM} - K_{Fuel,save}$	(Eq. 40)

Table 18
Specific costs for OPEX computation.

Name	Symbol	Value	Unit	Source
Specific O&M Costs	k_{OM}	2	%	Assumption
Specific Coal Costs	k_{coal}	90	EUR/t	Assumption

F. Pie chart of the CAPEX for the investigated cases.

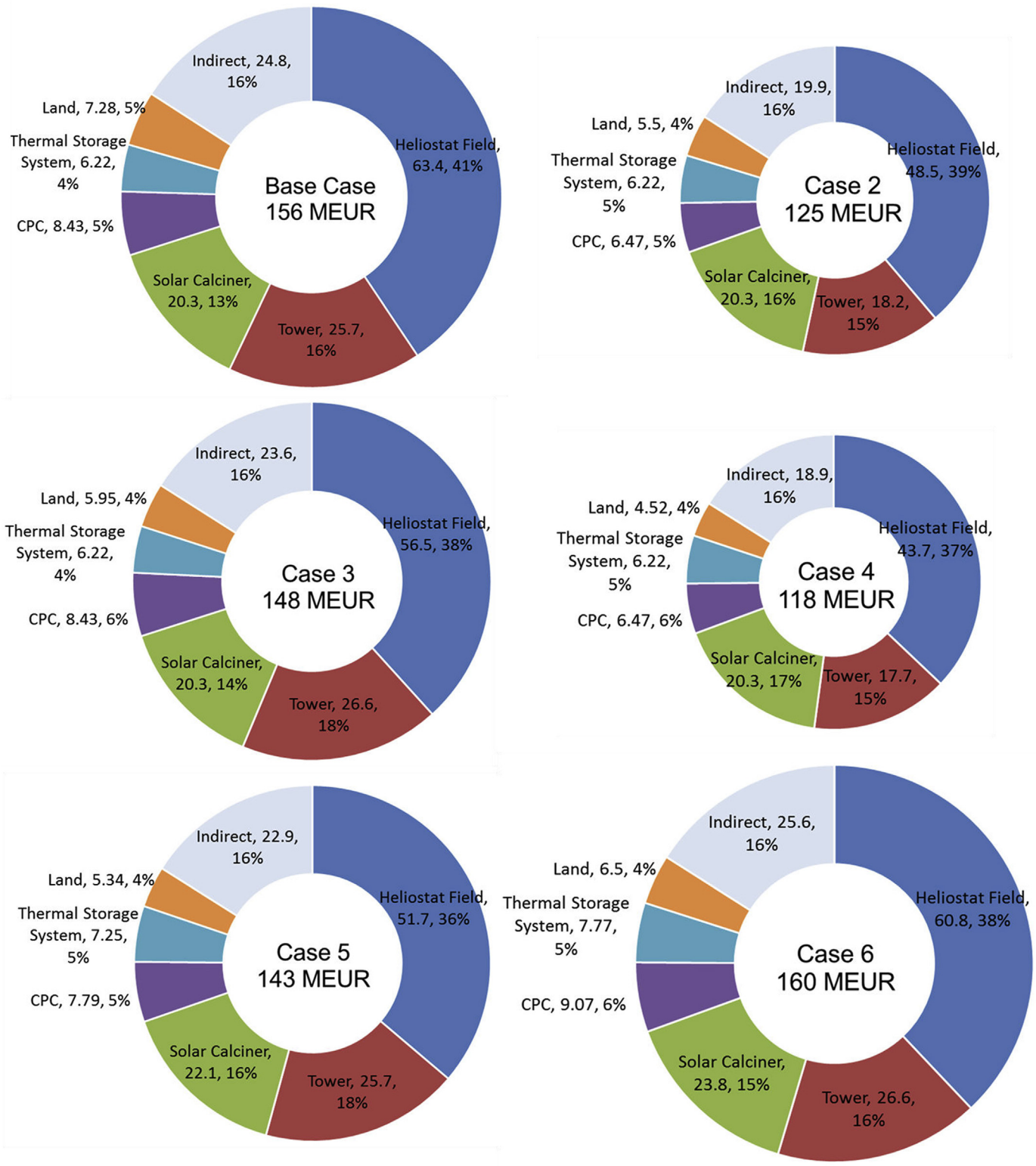

Fig. 18. CAPEX for the investigated cases of a solar cement plant in [MEUR].

References

[1] J.G.J. Olivier, et al., *Trends In Global CO_2 Emissions: 2016 Report*, 2016.
[2] M. Fischedick, et al., Industry, in: O. Edenhofer, et al. (Eds.), Climate Change 2014: Mitigation of Climate Change. Contribution of Working Group III to the Fifth Assessment Report of the Intergovernmental Panel on Climate Change, Cambridge University Press, Cambridge, United Kingdom, 2014.
[3] EUJRC Best available techniques (BAT) reference document for the production of cement, lime and magnesium oxide, in JRC Reference Reportreport,http://eippcb.jrc.ec.europa.eu/reference/BREF/CLM_Published_def.pdf2013.
[4] S. Sprung, Cement, in Ullmann's Encyclopedia Of Industrial Chemistry, 2008.
[5] J.A.H. Oates, Lime And Limestone : Chemistry and Technology, Production and Uses, Wiley-VCH, Weinheim; New York, 1998.
[6] R. Sebastián González, G. Flamant, Technical and economic feasibility analysis of using concentrated solar thermal technology in the cement production process: hybrid approach—a case study, J. Sol. Energy Eng. 136 (2) (2014), 025001.
[7] E.E.E. AG, *European Emission Allowances Auction (EUA) Primary Market*. 2018 [cited 2018 December 21st], Available from: https://www.eex.com/en/market-data/environmental-markets/auction-market/european-emission-allowances-auction.
[8] A. Meier, N. Gremaud, A. Steinfeld, Economic evaluation of the industrial solar production of lime, Energy Convers. Manag. 46 (6) (2005) 905–926.
[9] A. Meier, et al., Solar chemical reactor technology for industrial production of lime, Sol. Energy 80 (10) (2006) 1355–1362.
[10] R.S. González, G. Flamant, Technical and economic feasibility analysis of using concentrated solar thermal technology in the cement production process: hybrid approach—a case study, J. Sol. Energy Eng. 136 (2) (2014), 025001.
[11] R. Pitz-Paal, et al., Solar thermal power production, in: D. Stolten, V. Scherer (Eds.), Transition to Renewable Energy Systems, 2013.
[12] M. Ryssel, Carbon Dioxide Emission Reductions in the Cement Industry by Integrating Solar Calciner and CCUS Technologies, 2018 (RWTH-Aachen: Master thesis).
[13] G. Moumin, et al., Experimental And Theoretical Assessment Of a Solar Thermal Calcination Reactor, 04. Nov. 2016, 2. Workshop FT3 Gemeinsame Initiative Energiesystem 2050: Frankfurt am Main, Deutschland.
[14] G. Moumin, et al., Solar treatment of cohesive particles in a directly irradiated rotary kiln, Sol. Energy 182 (2019) 480–490.
[15] G. Flamant, et al., *Experimental aspects of the thermochemical conversion of solar energy; Decarbonation of $CaCO_3$*, Sol. Energy 24 (4) (1980) 385–395.
[16] A. Steinfeld, A. Imhof, D. Mischler, Experimental investigation of an atmospheric-open cyclone solar reactor for solid-gas thermochemical reactions, J. Sol. Energy Eng. 114 (3) (1992) 171–174.
[17] A. Imhof, Solar Cement Plants - an interesting challenge for business and science, ZKG Int. 53 (8) (2000) 448–457.
[18] A. Meier, et al., Design and experimental investigation of a horizontal rotary reactor for the solar thermal production of lime, Energy 29 (5–6) (2004) 811–821.
[19] S. Abanades, L. André, Design and demonstration of a high temperature solar-heated rotary tube reactor for continuous particles calcination, Appl. Energy 212 (2018) 1310–1320.
[20] IRENA, IEA-ETSAP, Concentrating Solar Power, Technology Brief, 2013.
[21] S. Dieckmann, et al., LCOE reduction potential of parabolic trough and solar tower CSP technology until 2025, AIP Conference Proceedings 1850 (1) (2017) 1–8.
[22] H. von Storch, Methanol Production via Solar Reforming of Methane, RWTH Aachen, Dissertation, 2016.
[23] A. Imhof, Calcination of limestone in a solar reactor, ZKG Int. 53 (9) (2000) 504–509.
[24] NREL. Concentrating Solar Power Projects, https://solarpaces.nrel.gov/. 2018 03/05/2018].
[25] CEMCAP, CO2 Capture from Cement Production. D4.2 Design and Performance of CEMCAP Cement Plant with MEA Post Combustion Capture, in https://www.sintef.no/globalassets/sintef-energi/cemcap/d4.2-design-and-performance-of-cemcap-cement-plant-with-mea-post-combustion-capture_rev1~1.pdf2016.
[26] CEMCAP, CO2 Capture from Cement Production. D3.2 CEMCAP Framework for Comparative Techno-Economic Analysis of CO2 Capture from Cement Plants, in https://www.sintef.no/globalassets/sintef-energi/cemcap/d3.2-cemcap-framework-for-comparative-techno-economic-analysis-of-co2-capture-from-cement-plants_.pdf2017.
[27] P. Schwarzbözl, M. Schmitz, R. Pitz-Paal, Visual HFLCAL - A Software Tool for Layout and Optimisation of Heliostat Fields, 2009.
[28] P. Schwarzbözl, The User's Guide to HFLCAL. A Software Program for Heliostat Field Layout Calculation, DLR, Cologne, 2009.
[29] Plataforma Solar de Almeria. Homepage. http://www.psa.es/en/ 2018; Available from: http://www.psa.es/en/index.php.
[30] OFICEMEN. Fábricas en España, Arraigadas en el territorio. https://www.oficemen.com/el-cemento/fabricas-cemento-espana/2018.
[31] R. Meyer, M. Schwandt, Documentation of Meteorological Data Sets Delivered Together with the SolarPACES Guideline for Bankable STE Yield Assessment, 2017.
[32] SolarPaces, SolarPACES *Guideline For Bankable STE Yield Assessment*. 15/06/2018, Available from: http://www.solarpaces.org/csp-research-tasks/task-annexes-iea/task-i-solar-thermal-electric-systems/solarpaces-guideline-for-bankable-ste-yield-assessment/.
[33] D. García-Gusano, H. Cabal, Y. Lechón, Long-term behaviour of CO2 emissions from cement production in Spain: scenario analysis using an energy optimisation model, J. Clean. Prod. 99 (2015) 101–111.
[34] OFICEMEN, Anuario del Sector Cementero Espanol, 2016. https://www.oficemen.com/wp-content/uploads/2017/07/Anuario-2016.pdf, 2017.
[35] Solargis, Solar resource maps of Spain, in https://solargis.com/maps-and-gis-data/download/spain/2017.
[36] O. Labahn, B. Kohlhaas, in: Cement Engineer's Handbook, 4 ed, Bauverlag, Wiesbaden, 1983.
[37] D.E. Garrett, Chemical Engineering Economics [E-Book], Springer Netherlands, Dordrecht, 1989, p. 432 (online resource).